CLIMATE CHANGE MODELLING FOR THE SOUTHERN REGION OF WESTERN AUSTRALIA

Rob Allan and Barrie Hunt

CSIRO Atmospheric Research

December 1999

CLIMATE CHANGE MODELLING FOR THE SOUTHERN REGION OF WESTERN AUSTRALIA

Rob Allan and Barrie Hunt

Published by CSIRO Atmospheric Research, Aspendale, Victoria, Australia.

ISBN 0 xxx xxxxx x

Contents

SUMMARY

Greenhouse-induced climatic change exists as a major problem worldwide. In this report a detailed assessment has been made of patterns of surface temperature and rainfall changes over south Western Australia (SWA). Results are presented from a number of international state-of-the–art global climatic models (GCM), as well as the CSIRO fine resolution regional model, DARLAM.

Results are compared from five GCMs which all used essentially the same scenario for the growth of atmospheric CO_2. Simulations were made with these models where aerosols (basically atmospheric particulates occurring due to the release of sulphur dioxide associated with the burning of fossil fuel, and mainly from Northern Hemisphere sources) were included or excluded. The inclusion of aerosols tends to cause a climatic cooling owing to the reflection of solar radiation. A comparison of the various simulations provides an indication of the sensitivity of climatic changes to the details of the design of the GCM, as there is no unique model formation. In addition, results are presented for the CSIRO Mark 2 GCM for three different CO_2 growth scenarios, again with and without increasing aerosols.

This combination of experiments provides a unique insight into the sensitivity of climatic change owing to both model formulation and the CO_2 scenario used, which have never been analysed previously for SWA.

The DARLAM results, based on one of the CSIRO simulations, then emphasise the improved detail and realism achievable by using finer horizontal resolution models.

The basic outcomes are as follows. By 2100, surface temperature increases of about 2-4.5°C can be expected in SWA, based on a consensus of the five GCM outputs. Slightly smaller increases occur if aerosols are included in the GCMs. A general drying over SWA is projected, with rainfall decreases of about 10-30% for winter-spring (JJA-SON) seasons by 2100. Again there is a range of possible outcomes across the various models, but there is overall less coherence in rainfall than in surface temperature simulations. Slightly smaller rainfall decreases occur when increasing aerosol levels are included in the GCMs.

Time series illustrating the year-by-year fluctuations in climate highlight the marked interannual variability in surface temperature and rainfall, which persist under greenhouse conditions. While the long term surface temperature increase is clearly apparent in these time series, rainfall changes are dominated by interannual variability.

The CSIRO Mark 2 GCM results for three CO_2 increase scenarios demonstrate the impact of CO_2 concentrations on climatic outcomes, with the more modest CO_2 amounts producing the smallest changes, as expected. Given the unknown future CO_2 growth scenarios, such an intercomparison is invaluable in clarifying potential climatic impacts.

INTRODUCTION

This report is produced under a contract with the Western Australian Environmental Protection Authority (EPA) on 'Climatic Modelling for the Southern Region of Western Australia'. Under this contract, an appraisal is made of the sensitivity of southwestern Australian (SWA) surface temperature and rainfall patterns under various enhanced greenhouse warming scenarios. This is achieved through the use of state-of-the-art transient coupled ocean-atmosphere global climatic model (GCM) and limited area model (DARLAM) simulations undertaken as part of CSIRO Atmospheric Research (CAR) and other international research programs.

GCMs replicate the basic details of the observed climate, with differences between them usually due to the manner in which they calculate some of the more intricate physical processes in the climate system. Transient GCM simulations are those in which greenhouse gases are allowed to build up in the model atmosphere in a way that mimics the observed atmospheric trend.

In all, five GCMs are examined. These are from the Canadian Climate Center (CCC), the Hadley Centre for Climatic Prediction and Research (HADCM2) in the United Kingdom, the Max-Planck Institute (MPI) for Meteorology in Germany, the Geophysical Fluid Dynamics Laboratory (GFDL) in the United States, and CSIRO (the CSIRO Mark 2 GCM). Finer spatial resolution in the horizontal plane, down to dimensions of 125 km over SWA, is achieved using the DARLAM nested within the CSIRO Mark 2 GCM. DARLAM is the only source available for fine resolution studies of this region.

Sensitivity of SWA climate to variations in GCM simulations is explored in the above range of models run under transient forcing conditions. All the runs simulate the effect of increasing atmospheric CO_2 concentrations, but in addition the effect of including (or not including) projected increases in sulphate aerosols is explored, as is the effect of variations in the rate of CO_2 increase. Increasing atmospheric aerosol concentrations into the next century are suggested by published reports of the Intergovernmental Panel on Climate Change (IPCC) (IPCC, 1996), although this is quite uncertain. New evidence indicates possible decreases towards the latter part of next century.

Table 1: Details of the GCM runs used in this report. (note only model results from 1961 onwards are shown in this report)

Centre	Model	Emission Scenario	Features	Years
Hadley Centre, UK[5]	HADCM2	1% CO_2 pa	Non-aerosol & Aerosol	1861-2100
CSIRO, Australia[1]	Mk2	IS92a equivalent CO_2	Non-aerosol & Aerosol	1881-2100
CSIRO, Australia[2]	Mk2	BAU & PL equivalent CO_2	Non-aerosol & Aerosol	1881-2100
GFDL[3]	GFDL CGCM	1% CO_2 pa	Non-aerosol & Aerosol	1958-2057
DKRZ, Germany (MPI runs)[4]	ECHAM4/OPYC3	IS92a	Non-aerosol & Aerosol	1860-2099
Canadian CCMA[6]	CGCM1	1% CO_2 pa	Non-aerosol & Aerosol	1900-2100

[1]Gordon and O'Farrell (1997)
[2]Dix (1999, per. com.)
[3]See http://ipcc-ddc.cru.uea.ac.uk/index.html
[4]DKRZ-Model User Support Group (1992), Oberhuber (1992)
[5]Cullen (1993)
[6]Flato et al. (submitted)

Recommendations for future research are detailed and examined in the final section of the report.

INTERCOMPARISON OF FIVE TRANSIENT GCM SIMULATIONS FOR SOUTH WESTERN AUSTRALIA: NON-AEROSOL AND AEROSOL CASES

Any particular GCM simulation of climate does not encompass all of the possible climatic changes that might occur, as the manner in which the physical processes are incorporated into GCMs is not unique. It is therefore valuable to compare the climatic simulations from a range of transient GCMs in order to obtain an estimation of the possible climatic changes associated with enhanced greenhouse warming.

In this part of the report, the climatic simulations presented are those generated by five international climate modelling groups using GCMs to examine enhanced greenhouse conditions. These experiments involve the use of similar transient CO_2 growth scenarios, both with and without increasing atmospheric aerosols. The horizontal resolution of these GCMs is of the order 250-500 kms at the equator, and decreases in size towards the poles.

a. Patterns of mean seasonal changes: Non-aerosol

The results of five international GCM simulations of the geographical distributions of seasonal mean surface temperature changes SWA for the periods 2010-2039, 2040-2069 and 2070-2099 (with respect to the 1961-2000 base period climatology) can be seen in Figures 1-5. The seasonal means constructed are for autumn (MAM), winter (JJA), spring (SON) and summer (DJF). It should be noted that the above epochs are 30-year period patterns at the beginning, in the middle, and at the end of the overall enhanced greenhouse warming. The GFDL simulations have only been run out to 2056, thus the GFDL GCM results are restricted to the 2010-2039 epoch and the first half of the 2040-2069 epoch.

Surface temperature

In Figures 1-5 (summarized in Table 2), all of the GCM simulations display future warming over Australia, with the most coherent patterns being seen in the 2040-2069 and 2070-2099 epochs. All of the GCM results indicate that the strongest surface temperature increases over Western Australia occur by the 2070-2099 period, and are most pronounced in the summer to autumn (DJF-MAM) seasons in the MPI and HADCM2 runs. Surface temperature increases over SWA are on the margins of the highest changes that occur over all, or parts, of inland Western Australia in any season. In general, most GCM simulations show an 0.5-1.6°C increase in all seasons in the 2010-2039 period, this rises to a 1.3-3.2°C increase in most seasons in the HADCM2, CCC and GFDL runs by the 2040-2069 epoch. By 2070-2099, the CCC, MPI and HADCM2 simulations have warming over SWA broadly in the range of 2-5.1°C, with the CCC results being more like 4.3-5.1°C. Of the models examined, the GFDL and CCC simulations show the most rapid seasonal surface temperature changes by the 2040-2069 period. The CCC and MPI GCM results show the strongest overall surface temperature change amongst the simulations between the 2010-2039 and 2070-2099 periods. More modest surface temperature increases occur in the CSIRO Mark 2 GCM.

The seasonal differentiation in surface temperature rises over SWA varies between models. The MPI, CAR and HADCM2 GCMs tend to show summer-autumn (DJF-MAM) peaks in warming, while the CCC simulation has a distinct winter-spring (JJA-SON) warming peak. In the 2040-2069 period, the HADCM2 and CAR simulations show the weakest warming over SWA. Most surface temperature variability is found in the MPI GCM patterns.

In summary, the GCMs show a consistent and growing surface temperature rise out to the year 2099. The range of surface temperature rise over SWA by the 2070-2099 epoch is of the order 2-5.1°C, with most model results being closer to 2.5°C.

Rainfall

Figures 6-10 (summarized in Table 3) show the percentage change in seasonal mean rainfall over SWA for each of the five GCMs. During the 2010-2039 epoch, there is a wide diversity in rainfall simulation patterns amongst the GCMs in any season. Generally, there is far more evidence of decreases than increases in seasonal mean rainfall over Western Australia amongst the GCM simulations. By the 2040-2069 period, all but the GFDL and CAR simulations suggest a decrease in SWA winter-spring (JJA-SON) rainfall of at least 20%. Only the CCC model indicates a distinct increase in summer (DJF) rainfall over SWA. In fact, the CAR and HADCM2 GCM results indicate a marked decrease in SWA summer (DJF) rainfall by 2070-2099, with the HADCM2 simulation showing a decrease of over 40%. Drying across SWA is strongest and most coherent by the 2070-2099 epoch in the HADCM2 simulation, while the CCC GCM results show some indications of increased rainfall in summer (DJF) during both the 2040-2069 and 2070-2099 periods. By 2070-2099, winter-spring (JJA-SON) rainfall decreases amongst the models are between 10-40%.

Overall, the SWA winter-spring (JJA-SON) rainfall decreases are generally seen as part of a wider reduction in rainfall in the Western Australian region. Only the CCC and CAR results include evidence for markedly increased summer-autumn (DJF-MAM) rainfall, mostly centred over northern parts of the State. The CCC GCM simulation has summer (DJF) increases of over 35% in both the 2040-2069 and 2070-2099 epochs.

b. Patterns of mean seasonal changes: aerosol

As with the non-aerosol GCM simulations, the results for the aerosol runs are performed by the same international models over the same periods/epochs and seasons. In these increasing aerosol simulations both the GFDL and MPI runs are restricted to results for only the first two epochs.

Surface temperature

The increasing aerosol simulations in Figures 11-15 indicate the various GCM seasonal patterns of surface temperature increases under enhanced greenhouse warming over Western Australia for the 2010-2039, 2040-2069 and 2070-2099 epochs. Once again, the SWA region is on the margins of the largest surface temperature changes that occur over inland Western Australia. As in the non-aerosol case, the CAR, MPI and HADCM2 simulations have their most pronounced surface temperature rise in the summer-autumn (DJF-MAM) seasons, while the CCC results show more of a winter-spring (JJA-SON) peak in warming. In the 2010-2039 period, the strongest surface temperature rises of 1-1.5°C are found in the CCC simulation and the weakest surface temperature rises of 0.5-1°C are seen in the MPI and CAR runs. By the 2040-2069 period, the strongest warming patterns of 2-3°C tend to be found in the CCC and GFDL simulations. The CCC GCM generates the strongest overall warming response in simulations with increasing aerosols by the 2070-2099 epoch. By the final period examined, warming amongst the models occurs in the range of 2-4.5°C.

Thus with increasing aerosols, enhanced greenhouse warming of surface temperatures over SWA in the GCMs is of the order of 2-4.5°C, i.e. somewhat less than in the non-aerosol runs.

Rainfall

As with non-aerosol GCM simulations, there is a general tendency for reduced rainfall over SWA in the GCM results with increasing aerosols (Figures 16-20). The 2010-2039 epoch shows a wide diversity in rainfall simulation patterns amongst the GCMs in any season. The strongest and most coherent rainfall decreases of 30-40% over SWA occur during the 2070-2099 period in the HADCM2 runs, especially in the winter-spring (JJA-SON) seasons. The remaining GCM simulations have various reduced rainfall patterns, but with quite mixed nature.

Rainfall increases are strongest and most coherent in summer (DJF) for the 2040-2069 and 2070-2099 epochs in the CCC simulations, where they are of the order of +40 to +60%. In fact, the CCC GCM results show the strongest contrast in rainfall tendency with dry winter (JJA) and wet summer (DJF) conditions.

To summarize, by 2070-2099 in the GCM simulations with increasing aerosols, rainfall decreases over SWA during the winter-spring (JJA-SON) seasons are of the order of 0-40%. In summer (DJF), model results indicate a wide range of rainfall tendencies by the 2070-2099 epoch of the order of –10 to +60%.

The above sets of results for the various GCMs illustrate present state-of-the-art simulations, and highlight current problems in producing a definitive answer attributable to enhanced greenhouse-induced climatic changes. When the CCC results are excluded there is more coherency between the GCM results, although seasonal differences still exist. To this extent, the overall projection for SWA is for warmer and drier conditions.

c. Mean seasonal tabulations of non-aerosol v aerosol changes

Tables 2 and 3 contrast the patterns of surface temperature and rainfall changes under enhanced greenhouse warming conditions for the various GCM simulations produced by non-aerosol and aerosol runs of the models across the land only portion of the SWA region.

Surface temperature

In Table 2, the contrast between non-aerosol and aerosol variants of the GCM simulations of surface temperature rises is generally small in the 2010-2039 and 2040-2069 epochs. However, by 2070-2099, all of the GCMs examined show various reductions in the rate of surface temperature rise under enhanced greenhouse warming conditions between the non-aerosol and aerosol runs. The largest reduction in the surface temperature rise across all seasons is found in the CCC and HADCM2 GCMs by 2070-2099.

Overall, the seasonal differences between non-aerosol and aerosol surface temperature rises are least in the CAR simulation, and most pronounced for the CCC and MPI GCM runs. Both the HADCM2 and CSIRO MARK 2 GCM runs show something of a preference in their seasonal warming patterns, with strongest surface temperature rises in summer-autumn (DJF-MAM) and weakest surface temperature rises in winter-spring (JJA-SON).

Overall, surface temperature rises by the 2040-2069 epoch common to all five GCMs are 0.2 to 1.2°C less in both winter-spring (JJA-SON) and summer-autumn (DJF-MAM) seasons in GCM runs with increasing aerosols.

Rainfall

Seasonal rainfall changes between the non-aerosol and aerosol GCM simulations are detailed in Table 3. Variations are not as consistent as for surface temperature and each GCM shows some seasons with increases and others decreases in rainfall changes between non-aerosol and aerosol experiments. By the 2070-2099 epoch, the strongest increases in summer (DJF) rainfall between non-aerosol and aerosol runs are found in the CCC GCM, while the strongest decreases in winter-spring (JJA-SON) are seen in the MPI and HADCM2 GCMs. The CCC and CSIRO MARK 2 GCMs show the most coherent retardation in percentage rainfall decreases between non-aerosol and aerosol runs in the 2070-2099 epoch. This is especially true in winter-spring (JJA-SON) and summer (DJF) seasons.

In summary, the difference in seasonal mean rainfall changes between aerosol and non-aerosols GCM simulations is small and mixed.

CHANGED CO_2 CONCENTRATION RUNS: CSIRO MARK 2 GCM RESULTS

More realistic transient-increasing atmospheric CO_2 changes for the 1870-2100 epoch have recently been used in CSIRO Mark 2 GCM simulations of climatic conditions under enhanced greenhouse warming. This approach also incorporates changes in atmospheric ozone (O_3), and involves simulations both with and without increasing atmospheric aerosols. In these simulations, two different increasing CO_2 concentrations are developed. To conform with the previous GCM analysis, results are calculated up to 2099.

Overall, these 'Business as usual' (BAU) and 'Policy Limited' (PL) scenarios for CO_2 change with time provide a useful contrast with the CO_2 change emission scenarios (see Table 1) used in the five international GCM simulations examined earlier (Figure 21).

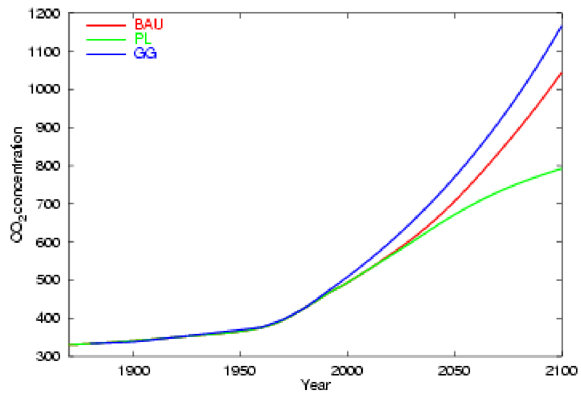

Figure 21: Greenhouse gases only GG (the IS92a emission scenario in Table 1), BAU and PL traces of CO_2 concentration over time used in the GCM simulations.

As can be seen in Figure 21 the BAU and PL CO_2 concentration curves only begin to diverge after about 2040, and thus the geographical patterns of the 2010-2039 surface temperature and rainfall change results are virtually identical in the non-aerosol and aerosol cases. Thus, discussion in this section focuses on the 2040-2069 and 2070-2099 epoch results.

c. Geographical distributions over SWA: Non-Aerosols

The spatial pattern of seasonal mean surface temperature and rainfall changes under BAU and PL scenarios over SWA for the non-aerosol GCM runs are shown in Figures 22 to 25.

Surface Temperature

In both the BAU and PL scenarios the rise in surface temperature over SWA in the 2040-2069 epoch is very similar, being in the range of 1.25-1.75°C (Figures 22 and 23). The only real difference in warming is found by the 2070-2099 period when the BAU scenario shows a surface temperature rise over SWA of the order of 2-2.5°C, while for the PL scenario it is around 1.5-2°C. Only the PL scenario suggests any seasonal difference in warming over Western Australia, with a winter (JJA) maximum by 2070-2099.

The differences between the BAU and PL results highlight the impact of changes in the assumed atmospheric CO_2 growth rate (compare also with Figure 1). Obviously, policies designed to minimise the net CO_2 emissions to the atmosphere will have an impact on the resultant climatic changes, and intercomparisons such as those shown in Figure 22 and 23 demonstrate the different outcomes.

Rainfall

As seen in other variants of the GCM simulations, the seasonal mean rainfall change patterns in Figures 24 and 25 are more mixed than those for surface temperature. The BAU scenario for the 2040-2069 epoch has rainfall changes over SWA ranging from –10 to +10%. Increased SWA rainfall is most evident in autumn (MAM) as part of the extension of enhanced rainfall conditions over most of inland Western Australia. The summer (DJF) season has the biggest decrease in rainfall over SWA. By contrast, the PL scenario indicates very mixed seasonal rainfall changes of low order.

By 2070-2099, the BAU scenario has a marked contrast in rainfall over Western Australia in summer (DJF). At this time, northern coastal regions show decreases of the order of 40-80%, while over SWA there are a mixture of very weak changes. In general however, the 2070-2099 seasonal rainfall change pattern is very mixed. This weak and incoherent nature of seasonal rainfall changes is also seen in the PL scenario in the 2070-2099 epoch.

Overall, the rainfall change picture by the 2070-2099 epoch is very mixed for both the BAU and PL scenarios. Strongest rainfall responses are found under the BAU scenario, especially in summer-autumn (DJF-MAM) seasons. In comparison with Figure 6, the results in Figure 24 and 25 reveal only modest consistency, thereby highlighting the sensitivity of the rainfall changes to the selected CO_2 scenario.

d. Geographical distributions over SWA: Aerosols

The spatial pattern of seasonal mean surface temperature and rainfall changes under BAU and PL scenarios over SWA for the GCM runs that include increasing aerosols are shown in Figures 26 to 29.

Surface Temperature

The inclusion of increasing aerosols in the BAU and PL GCM runs makes little difference to the surface temperature rises over SWA in these scenarios (Figures 26 and 27). As with the non-aerosol case, warming over SWA is of the order of 1.25-1.75°C in the 2040-2069 epoch. For Western Australia as a whole, the seasonality of the warming seems to favour a summer (DJF) maximum.

As in the non-aerosol case, the most coherent difference in seasonal mean surface temperature rise between the BAU and PL scenarios is evident by the 2070-2099 period. For the BAU run, warming over SWA at this time is around 2-2.75°C. This can be contrasted with a warming of between 1.5-2°C for the PL scenario. Again, there is some suggestion of a seasonal contrast in warming with highest seasonal mean surface temperature rises over inland Western Australia in summer-autumn (DJF-MAM).

The surface temperature increases for the 2070-2099 epoch are actually larger than those seen in the non-aerosol runs (Figures 22 and 23), because the assumed aerosol concentration is below that for the reference period 1961-2000. Implicit in the BAU and PL aerosol cases are major controls designed to reduce sulphate emissions to the atmosphere. Again, this illustrates the need to explore multiple CO_2 and sulphate emission scenarios to quantify possible future enhanced greenhouse-induced climatic changes.

In summary, by the 2070-2099 epoch, seasonal mean surface temperature rises over SWA under the PL scenario of CO_2 concentration changes in the increasing aerosol run are of the order of 0.5-0.75°C lower than for the BAU scenario.

Rainfall

The GCM aerosol simulations for the BAU scenario in the 2040-2069 epoch show decreased rainfall over SWA in spring-summer (SON-DJF) of the order of 20-40% (Figures 28 and 29). Rainfall for the other seasons is also reduced, but only marginally. As in the non-aerosol BAU scenario, the autumn (MAM) season shows enhanced rainfall conditions over most of inland Western Australia. In the PL scenario, reduced rainfall (of the order of 0-20%) is seen in all but the winter (JJA) season for the 2040-2069 epoch.

By the 2070-2099 period, rainfall is reduced over SWA in every season of the BAU scenario. Most pronounced SWA rainfall reductions occur in spring (SON), reaching values of 40% and more. As in the non-aerosol case, the PL scenario has very weak SWA rainfall tendencies by 2070-2099. Comparison with Figure 16 reveals very little consistency between the experiments.

Overall, the picture is one of rainfall reductions over SWA in most seasons. The only coherency in these patterns is in the spring-summer (SON-DJF) seasons of the 2040-2069 epoch during the BAU scenario, when rainfall decreases of up to 40% are found.

d. Time series of seasonal mean surface temperature and rainfall changes over SWA

Warming trends are evident in all of the seasonal mean surface temperature time series for BAU and PL CO_2 concentration scenarios in runs both with and without increasing aerosols in Figures 30-33. These traces confirm the results of the analysis of the spatial patterns of seasonal mean surface temperature over SWA above. There is little overall difference between the non-aerosol and aerosol runs within each of the wider and land only regions of SWA (Figure 38) for either the BAU or PL scenarios. Comparisons between BAU and PL scenario time series between the wider and land only regions of SWA tend to confirm the tendency for less warming under the PL scenario. The important feature of these figures is the year-to-year variability in surface temperature, thereby highlighting the necessity of viewing surface temperature variability over a decade or more to obtain a proper perspective of any temperature changes.

Figures 34-37 detail time series of seasonal mean rainfall changes for BAU and PL CO_2 concentration scenarios in runs both with and without increasing aerosols for the wider and land only regions of SWA. Both of the regions of SWA show a downward trend in rainfall during spring (SON) in the BAU increasing aerosol scenario for the latter half of the time period. For the wider SWA region this downward trend is evident in the wider winter-spring (JJA-SON) seasons. The PL non-aerosol and aerosol scenarios show a small downward trend in rainfall during winter-spring (JJA-SON) seasons for the latter half of the time period over the wider SWA region. A weak a downward trend in spring (SON) rainfall is still evident for the PL increasing aerosol case over the land only region of SWA.

Note the very high degree of interannual variability in the rainfall time series. This emphasises the problem of deducing overall trends from short period samples, either observed or modelled.

Overall, upward trends are evident in seasonal mean surface temperature in both the wider and land only areas of SWA. There is confirmation that under the PL scenario the rate of warming over time is less than for the BAU scenario. There is no change in the mean surface temperature range in any season over time.

A downward trend is most evident in the BAU increasing aerosol scenario in spring (SON) during the last half of the time series for both wider and land only regions of SWA.

125 KM HORIZONTAL RESOLUTION ANALYSIS FOR SOUTHERN WESTERN AUSTRALIA FROM THE DARLAM REGIONAL CLIMATIC MODEL

A fine resolution regional climate model (DARLAM) has been embedded in the existing CSIRO MARK 2 GCM enhanced greenhouse warming simulation (involving a transient-increasing atmospheric CO_2 concentration for the period 1960-2099), and used to calculate 125 km horizontal resolution fields of seasonal mean surface temperature and percentage changes in rainfall over SWA. Spatial patterns of changes in these parameters are displayed over the wider SWA area shown in Figure 38, while time series are generated for both the wider and land only regions of SWA.

a. Geographical distributions of seasonal mean surface temperature changes over SWA

Figure 39 shows the spatial distribution of seasonal mean surface temperature from the DARLAM simulation for the 2010-2039, 2040-2069 and 2070-2099 epochs, and can be compared to the CSIRO MARK 2 GCM results in Figure 1. Over SWA, the seasonal mean surface temperature increases from around 0.5-1.25°C in 2010-2039 up to between 2-2.75°C by 2070-2099. By the 2070-2099 epoch, there is a marked gradient in the warming pattern from lowest values over SWA to the highest values over northern parts of Western Australia. In general, this DARLAM simulation begins to pick up more subtle structure in the pattern of surface temperature increase over SWA. By the 2040-2069 period, there are even suggestions of some coastal versus inland variations in surface temperature across the SWA region. Higher resolution results would greatly add to these features.

To summarize, the DARLAM (nested within the CSIRO MARK 2 GCM) simulation shows a seasonal mean surface temperature rise over SWA of around 2-2.75°C by the 2070-2099 epoch. The strongest SWA warming pattern is seen in the spring (SON) season. Overall, the range in SWA warming is almost identical to that seen in the CSIRO MARK 2 GCM, which was of the order of 2-2.65°C. However, the spatial pattern of seasonal mean surface temperature rise in DARLAM appears to show more realistic horizontal structure compared to the CSIRO MARK 2 GCM results across SWA.

b. Geographical distributions of seasonal mean rainfall changes over SWA

Seasonal mean rainfall changes over SWA in the DARLAM simulations in Figure 40 show a general tendency towards drying, and can be compared to the results from the CSIRO MARK 2 GCM in Figure 6. All seasons in the 2010-2039 period show varying degrees of enhanced rainfall over northern parts of Western Australia, with strongest increases in summer-autumn (DJF-MAM).

By the 2040-2069 epoch, most drying over SWA (around 10% rainfall decrease) is centered on the winter (JJA) season. Increases are again evident further north over the State, extending into SWA in summer (DJF). The spring (SON) pattern of rainfall shows drying over the whole of the domain, but with the strongest drying centered in the north of the State.

The final period examined in this study (2070-2099) details a pattern of extensive drying (of the order of 20%) over SWA in winter-spring (JJA-SON) seasons. Only the summer (DJF) season shows an increase in rainfall.

A number of differences are apparent between the rainfall changes in Figures 6 and 40. The higher resolution DARLAM results would in general be considered to be more representative of reality, although much higher resolution is desirable.

In summary, rainfall decreases in the DARLAM simulation are of the order of 20% over SWA in winter-spring (JJA-SON) seasons by 2070-2099. During summer (DJF), increases of 0 to +20% across the region are most evident in the 2040-2069 epoch. In contrast, the CSIRO MARK 2 GCM runs show a summer (DJF) decrease in rainfall over SWA of around 23%, and an autumn-spring (MAM-SON) rainfall change ranging from +8% to –29% by 2070-2099. Thus the DARLAM results are similar to the CSIRO MARK 2 GCM findings in winter (JJA) but wetter in summer (DJF).

c. Time series of seasonal mean maximum and minimum surface temperature changes over SWA

Figure 41 shows time series of the seasonal mean maximum surface temperature from the DARLAM simulation for both the wider and land only regions of SWA detailed in Figure 38. All seasons for both regions of SWA indicate an upward trend in maximum surface temperature. There is no indication of the trend being stronger in either of the SWA regions shown. On shorter time scales, all time series show fluctuations in seasonal mean maximum surface temperature in the range of 4-6°C, especially in the autumn (MAM) season. There is no obvious change in the maximum surface temperature range in any season over the period of the DARLAM simulation. These time series indicate how the simulated changes in mean climate could be manifest against the background natural variability in the climate system. The figure also provides an indication of the more likely occurrence of extreme surface temperatures under enhanced greenhouse conditions, which can have serious impacts.

Seasonal mean minimum surface temperature time series in Figure 42 also show an upward trend for both the wider and land only regions of SWA. For this parameter, seasonal mean minimum surface temperature over the wider SWA region is noticeably higher in value than for the smaller, land only SWA area. As with the seasonal mean maximum surface temperature time series, there is no change in the minimum surface temperature range in any season over the period of the DARLAM simulation.

In summary, upward trends are evident in both seasonal mean maximum and minimum surface temperature but there is no change in the range of these parameters over time.

d. Time series of seasonal mean rainfall changes over SWA

The seasonal mean rainfall time series and trend lines (3rd order polynomial fit to the data) in Figure 43 show very similar overall rainfall responses for both the wider and land only regions of SWA. Large overall trends are not readily evident in any season, although there is evidence for a downward tendency in rainfall over the land only region of SWA for the winter and spring (JJA-SON) seasons, which matches that seen in the seasonal mean spatial patterns of rainfall. There is certainly some suggestion of shorter epoch trends of the order of 20-30 years duration in all seasons within the full rainfall time series.

Overall, there is evidence of a small downward trend in rainfall over the land only region of SWA for the winter and spring (JJA-SON) seasons.

CONCLUSIONS

The results presented in this report have been designed to display the range of possible climatic changes that might be expected over SWA associated with the enhanced greenhouse effect. For conciseness, the analysis has been restricted to the two important climatic variables: surface temperature and rainfall. Thus, climatic changes have been presented for five different GCMs using essentially the same CO_2 growth scenario, both with and without increasing aerosol affects included, thereby indicating the sensitivity of outcomes to the individual GCM formulations. In addition, for the CSIRO Mark 2 GCM three different CO_2 growth scenarios, again both with and without increasing aerosols, have been presented to highlight the impact on climatic change of the choice of CO_2 scenario. Finally, results have been given for one CSIRO simulation using enhanced horizontal resolution via the DARLAM model, to illustrate the greater detail and sensitivity associated with such models.

All experiments indicate an overall warming can be expected in SWA in the future owing to the enhanced greenhouse effect. For the multiple GCM CO_2 scenario the consensus outcome is for a surface temperature increase of the order of 2.5°C for the non-aerosol case by the year 2100. A slightly smaller increase was obtained when increasing aerosols were included in the GCMs. As demonstrated with the multiple CSIRO simulations, the surface temperature increases are sensitive to both the CO_2 and aerosol emission scenarios used, with the more modest CO_2 increases associated with the PL scenario producing the lowest surface temperature rises.

Currently, there is no consensus on which CO_2 growth scenario will prevail, and the range of results presented here provides a valuable perspective of possible surface temperature increases.

As expected, there was less consistency between the various model simulations as regards rainfall changes under enhanced greenhouse conditions. Excluding the results from the CCC GCM, which appears to be an outlier, then the overall tendency across the GCMs is for a decline in rainfall. The results are succinctly summarised in Table 3. For the critical winter-spring (JJA-SON) seasons, where SWA rainfall is at a maximum, there was an overall consensus amongst the various GCMs for a reduction in rainfall of about 10-30% by 2100 for non-aerosol conditions, and slightly less when aerosols were included (see Table 3).

Across all of the simulations the amplitude of the enhanced greenhouse signals increased with time as the impact of the increasing CO_2 concentrations was felt.

The time series showing the temporal changes in surface temperature and rainfall for SWA highlight the considerable interannual variability that continued to occur under enhanced greenhouse conditions. Nevertheless, the inexorable rise in surface temperature is clearly displayed, although the more modest increases associated with the PL scenario again emphasise the importance of the choice of CO_2 emission rate. In the case of rainfall, the time series were dominated by interannual variability, and downward trends were visible for winter-spring (JJA-SON) only late next century.

The potential improvement in simulation details of the climatic changes is indicated with outputs from the DARLAM regional model. Nevertheless, much higher resolution is clearly required to capture regional outcomes. The time series of maximum surface temperatures from DARLAM herald a critical problem expected to emerge under enhanced greenhouse conditions. This is the inevitable increase in daily maximum surface temperatures, such that values only occasionally experienced at present become more typical. Inevitably, a range of heat stress related issues will occur.

Of necessity, only a brief sample of possible climatic changes have been documented here. Numerous other issues still require analysis, such as the expected decline in soil moisture content resulting from higher evaporation rates due to the increased surface temperature, coupled with lower rainfall. Impacts on the agricultural sector and water supplies can obviously be expected.

RECOMMENDATIONS FOR FUTURE RESEARCH

There is a need to simulate climatic change using improved GCMs and subsequently enhancing their outputs by running regional models such as DARLAM at far higher horizontal resolution than was possible in this report. The CSIRO Mark 3 GCM is now becoming available for climatic research and, in assessments to date, has demonstrated a considerable improvement in its simulation capabilities. DARLAM runs at 60 km, or finer, resolution using CSIRO Mark 3 GCM outputs offer the capability of achieving unprecedented quality results.

Some of the practical tasks that could be undertaken include:

- More detailed examinations of surface temperature changes, including quantification of the number of days above a given maximum surface temperature threshold, and the increase in this number with time.
- More precise delineation of rainfall changes, including changes in maximum rainfall rates, return periods, changes in the frequency and duration of dry episodes.
- An assessment of the implications of climatic change with regard to water supply security.
- Linking up climatic changes to other scientific groups with knowledge in health issues, urban services, wildlife requirements, forestry etc.
- Quantification of changes to tropical cyclone events.
- The interactions between climatic change and naturally occurring climatic variability.

ACKNOWLEDGEMENTS

The authors would like to thank Ms Cher Page and Ms Janice Bathols for their work on processing the various model data and constructing the bulk of the diagrams and figures. Additional thanks go to Dr Martin Dix for the BAU and PL analysis data and Figure 21, Dr Kevin Walsh for providing the basis for Table 1, and Dr Ramasamy Suppiah for aiding in the processing of several of the time series.

REFERENCES

Cullen, M.J.P. (1993) The unified forecast/climate model. *Meteorological Magazine*, **122**, 81-94.

DKRZ-Model User Support Group (eds) (1992) *ECHAM3 - Atmospheric General Circulation Model*. Report No. 6, Deutsches Klimarechenzentrum, Hamburg. http://www.dkrz.de/forschung/reports/ReportNo.6.ps

Flato, G.M., Boer, G.J., Lee, W.G., McFarlane, N.A., Ramsden, D., Reader, M.C. and Weaver, A.J. (submitted) The Canadian Centre for Climate Modelling and Analysis Global Coupled Model and its Climate, submitted to *Climate Dynamics*.

Gordon, H.B. and O'Farrell, S.P. (1997) Transient climate change in the CSIRO coupled model with dynamic sea ice. *Monthly Weather Review*, **125**, 875- 907.

IPCC, 1996: *Climate Change 1995: The Science of Climate Change.* Houghton, J.T., Meira Filho, L.G., Callander, B.A., Harris, N., Kattenberg, A. and Maskell, K. (eds), Contribution of Working Group 1 to the second assessment report of the Intergovernmental Panel on Climate Change, Cambridge University Press, Cambridge, 572 pp.

Oberhuber, J.M. (1992) *The OPYC Ocean General Circulation Model*. Report No. 7, Deutsches Klimarechenzentrum, Hamburg. http://www.dkrz.de/forschung/reports/Report No.7.ps

TABLES

TABLE 2: GCM SEASONAL WARMINGS (°C) OVER SOUTH WESTERN AUSTRALIA (LAND ONLY REGION IN FIGURE 38) WITH REGARD TO THE 1961-2000 CLIMATOLOGY FOR NON-AEROSOL (na) AND AEROSOL (a) RUNS

MODELS	MAM	JJA	SON	DJF
CCC-na				
2010-2039	1.5	1.2	1.6	1.4
2040-2069	2.7	2.7	3.2	2.9
2070-2099	4.3	4.6	5.1	4.6
CCC-a				
2010-2039	1.3	1.3	1.4	1.1
2040-2069	2.1	2.3	2.9	2.1
2070-2099	3.3	3.9	4.5	3.4
HADCM2-na				
2010-2039	1.1	1.0	1.2	1.1
2040-2069	2.4	1.8	2.0	2.1
2070-2099	3.7	2.7	2.8	3.6
HADCM2-a				
2010-2039	0.8	0.8	0.9	0.8
2040-2069	1.5	1.2	1.5	1.9
2070-2099	2.8	2.4	2.5	3.0
GFDL-na				
2010-2039	1.3	1.6	1.6	1.6
2040-2069	2.4	2.7	2.7	3.1
2070-2099				
GFDL-a				
2010-2039	1.0	1.2	1.2	1.6
2040-2069	2.1	2.0	2.5	2.1
2070-2099				
MPI-na				
2010-2039	1.0	0.8	0.8	1.1
2040-2069	1.6	1.4	1.4	1.7
2070-2099	2.4	2.1	2.3	2.8
MPI-a				
2010-2039	0.8	0.7	0.7	1.0
2040-2069	0.9	0.6	0.8	1.4
2070-2099				
CSIRO-na				
2010-2039	0.8	0.8	0.8	0.7
2040-2069	1.5	1.3	1.6	1.8
2070-2099	2.3	2.0	2.4	2.7
CSIRO-a				
2010-2039	0.7	0.7	0.7	0.5
2040-2069	1.5	1.4	1.5	1.5
2070-2099	2.1	2.0	2.1	2.1

TABLE 3: GCM PERCENTAGE CHANGES IN SEASONAL RAINFALL OVER SOUTH WESTERN AUSTRALIA (LAND ONLY REGION IN FIGURE 38)WITH REGARD TO THE 1961-2000 CLIMATOLOGY FOR NON-AEROSOL (na) AND AEROSOL (a) RUNS (Positive increments > 20% are shaded %; negative increments < 20% are shaded %)

MODELS	MAM	JJA	SON	DJF
CCC-na				
2010-2039	16	-14	-13	22
2040-2069	2	-27	-28	35
2070-2099	-3	-36	-26	40
CCC-a				
2010-2039	-15	-9	-11	10
2040-2069	-10	-15	-14	41
2070-2099	0	-26	-16	63
HADCM2-na				
2010-2039	-27	-30	-8	0
2040-2069	-34	-31	-22	-22
2070-2099	-39	-36	-32	-48
HADCM2-a				
2010-2039	-9	-19	-15	-4
2040-2069	-5	-24	-30	-21
2070-2099	-32	-42	-31	-35
GFDL-na				
2010-2039	5	-8	-3	-3
2040-2069	12	0	-17	-4
GFDL-a				
2010-2039	7	-6	-11	-11
2040-2069	-4	-5	-17	0
MPI-na				
2010-2039	-9	-24	-22	-10
2040-2069	-27	-27	-34	-13
2070-2099	-28	-40	-36	-14
MPI-a				
2010-2039	-12	-13	-19	-2
2040-2069	-20	-33	-36	-6
CSIRO-na				
2010-2039	-1	-4	-2	1
2040-2069	-8	-10	-19	2
2070-2099	8	-13	-28	-23
CSIRO-a				
2010-2039	9	-8	-11	3
2040-2069	-12	-12	-16	17
2070-2099	-7	-1	-16	-10

FIGURES

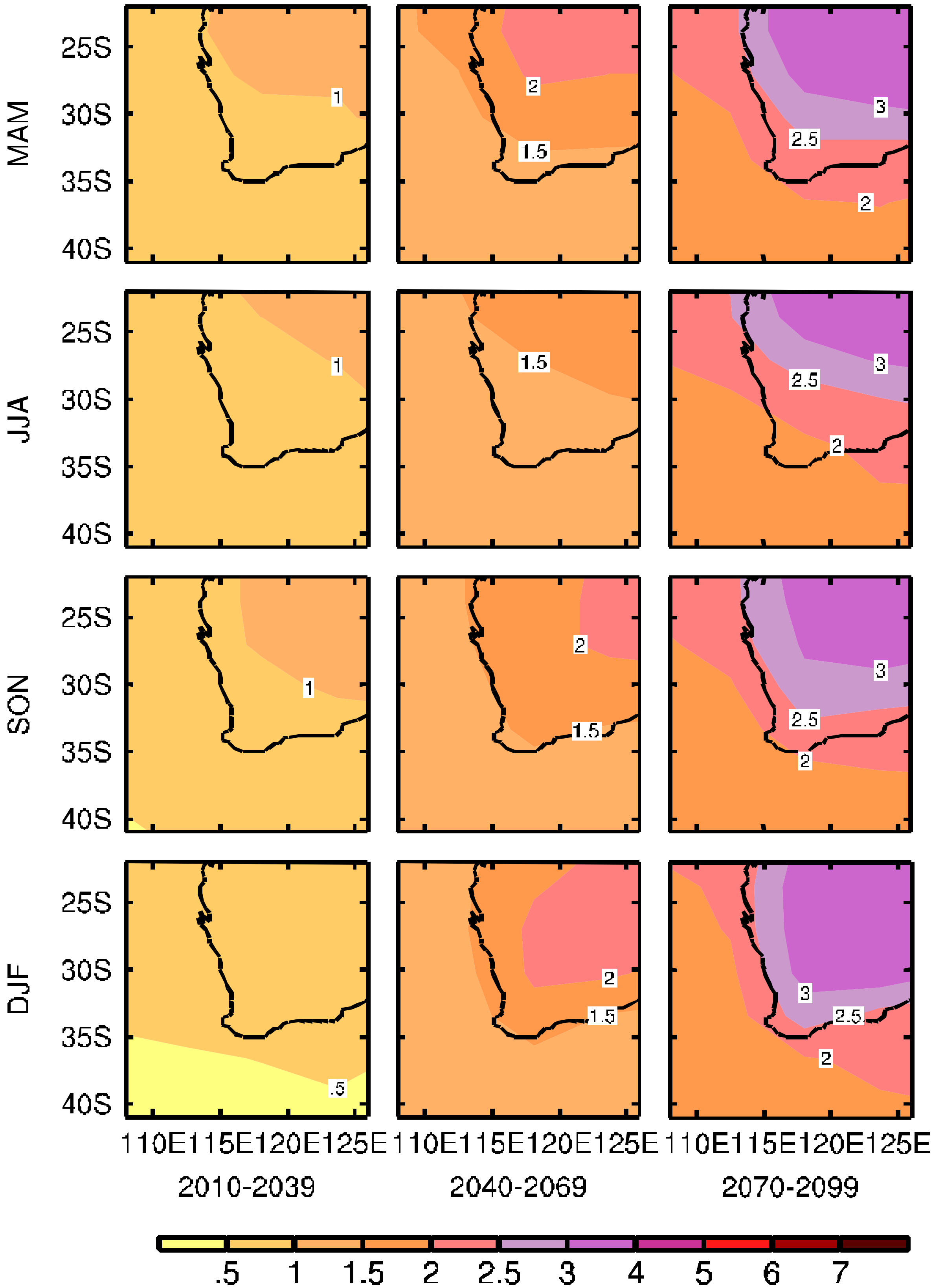

Figure 1: Non-aerosol CSIRO MARK 2 GCM simulations of seasonal mean surface temperature change over SWA in the 2010-2039, 2040-2069 and 2070-2099 epochs. Seasons are autumn (MAM), winter (JJA), spring (SON) and summer (DJF). Surface temperature is in °C, with the colour bar on the figure showing the surface temperature contour values.

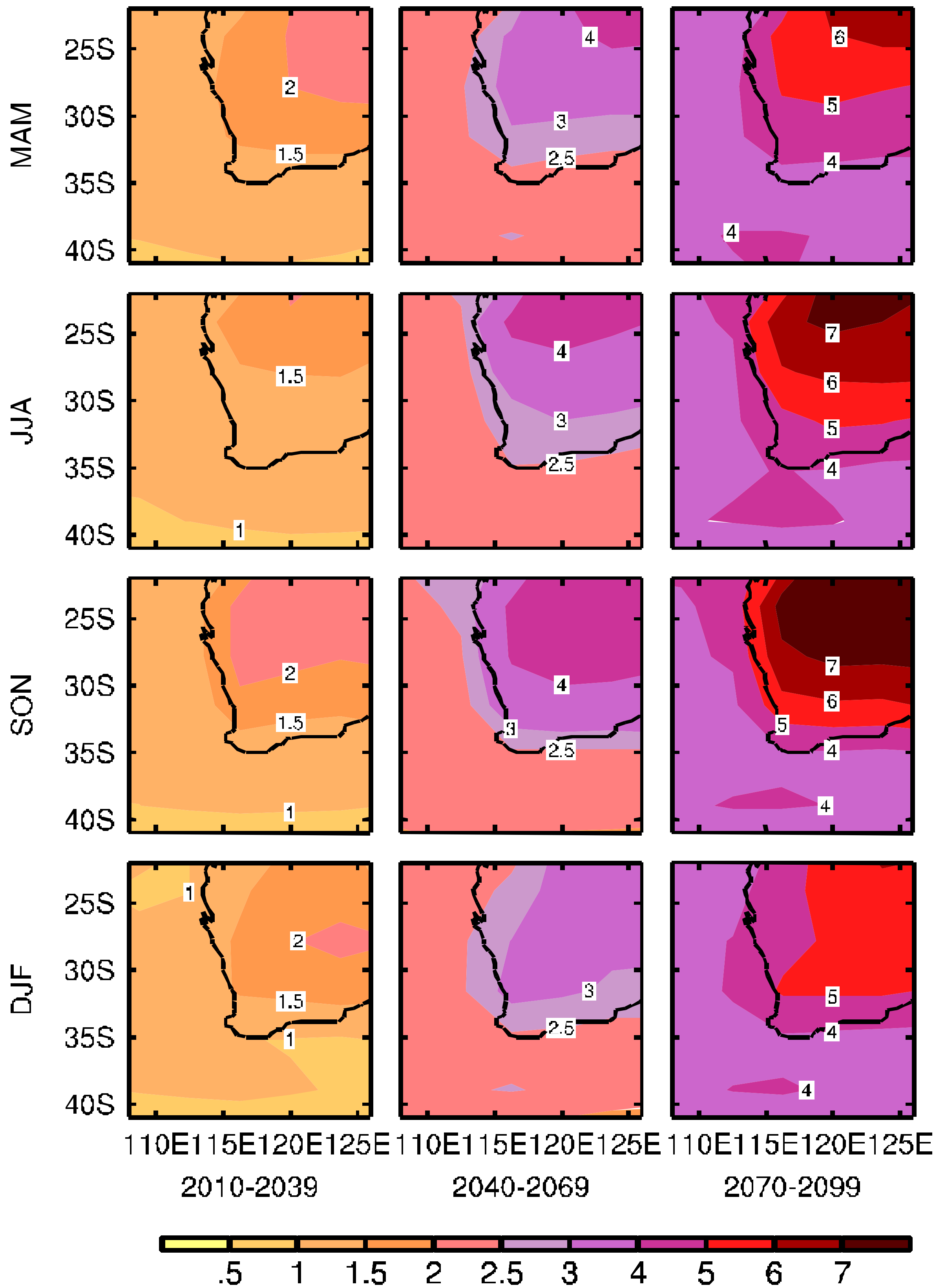

Figure 2: Non-aerosol CCC GCM simulations of seasonal mean surface temperature change over SWA in the 2010-2039, 2040-2069 and 2070-2099 epochs. Seasons are autumn (MAM), winter (JJA), spring (SON) and summer (DJF). Surface temperature is in °C from the 1961-2000 climatology, with the colour bar on the figure showing the surface temperature contour values.

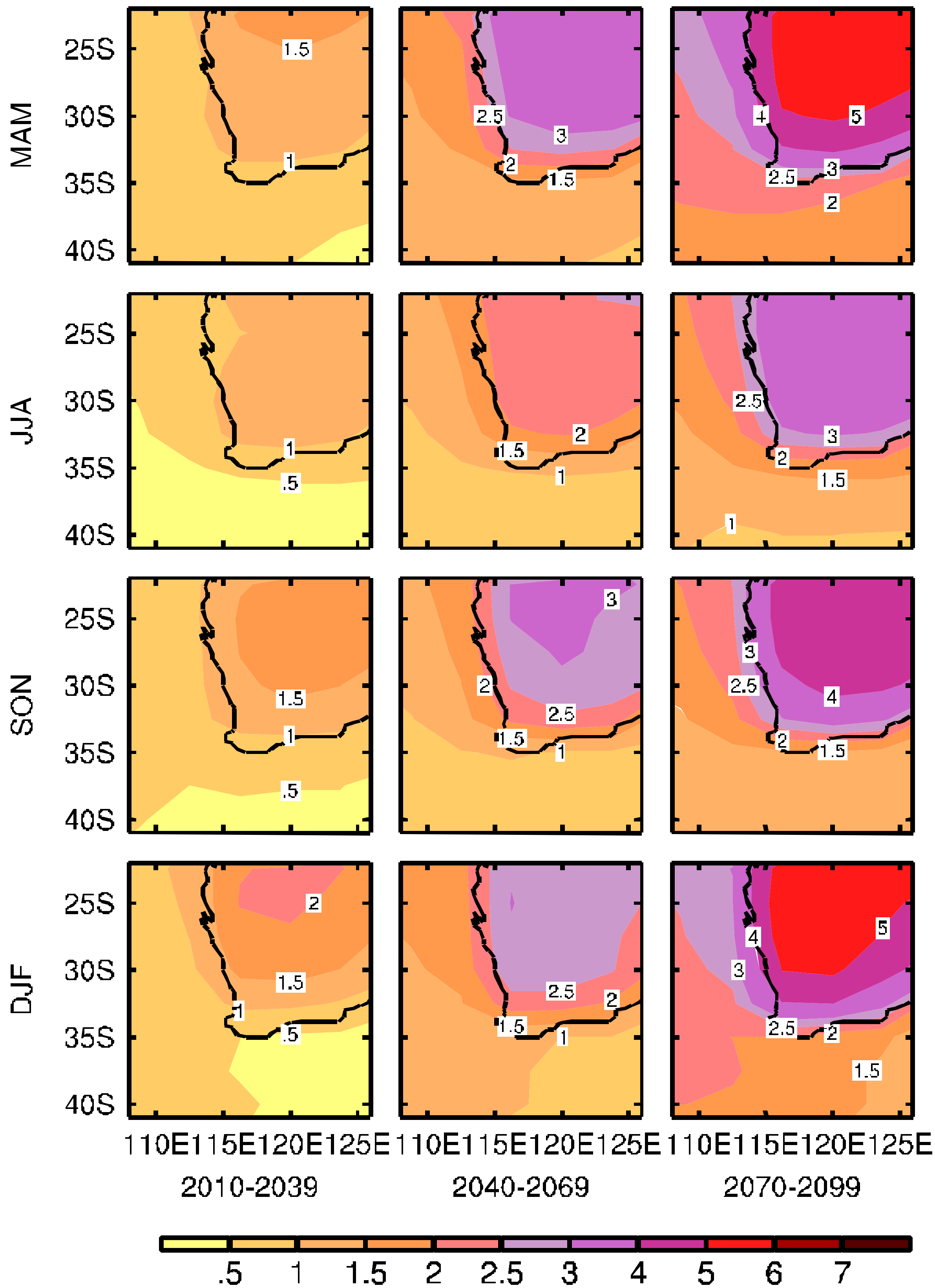

Figure 3: Non-aerosol HADCM2 GCM simulations of seasonal mean surface temperature change over SWA in the 2010-2039, 2040-2069 and 2070-2099 epochs. Seasons are autumn (MAM), winter (JJA), spring (SON) and summer (DJF). Surface temperature is in °C from the 1961-2000 climatology, with the colour bar on the figure showing the surface temperature contour values.

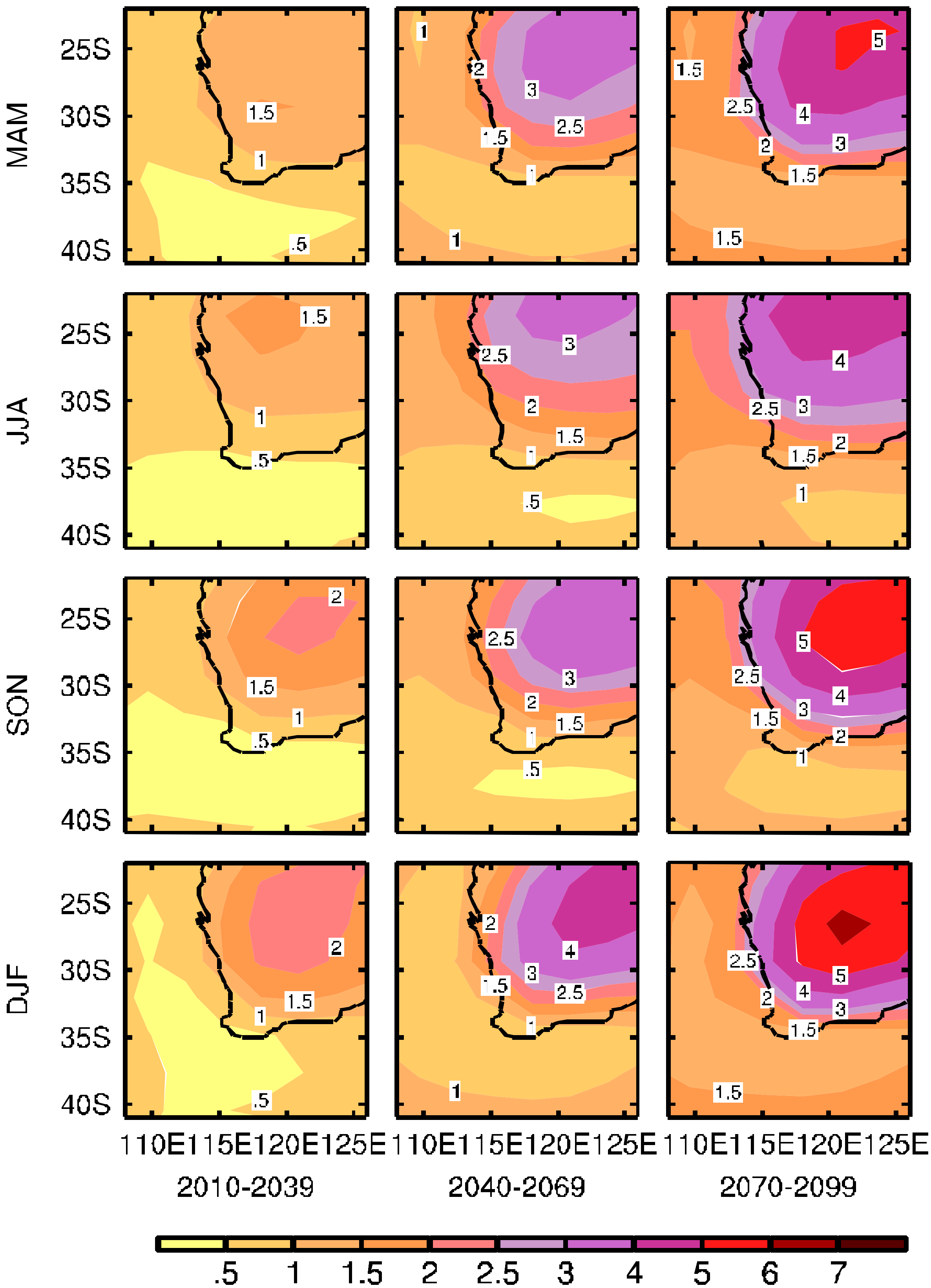

Figure 4: Non-aerosol MPI GCM simulations of seasonal mean surface temperature change over SWA in the 2010-2039, 2040-2069 and 2070-2099 epochs. Seasons are autumn (MAM), winter (JJA), spring (SON) and summer (DJF). Surface temperature is in °C from the 1961-2000 climatology, with the colour bar on the figure showing the surface temperature contour values.

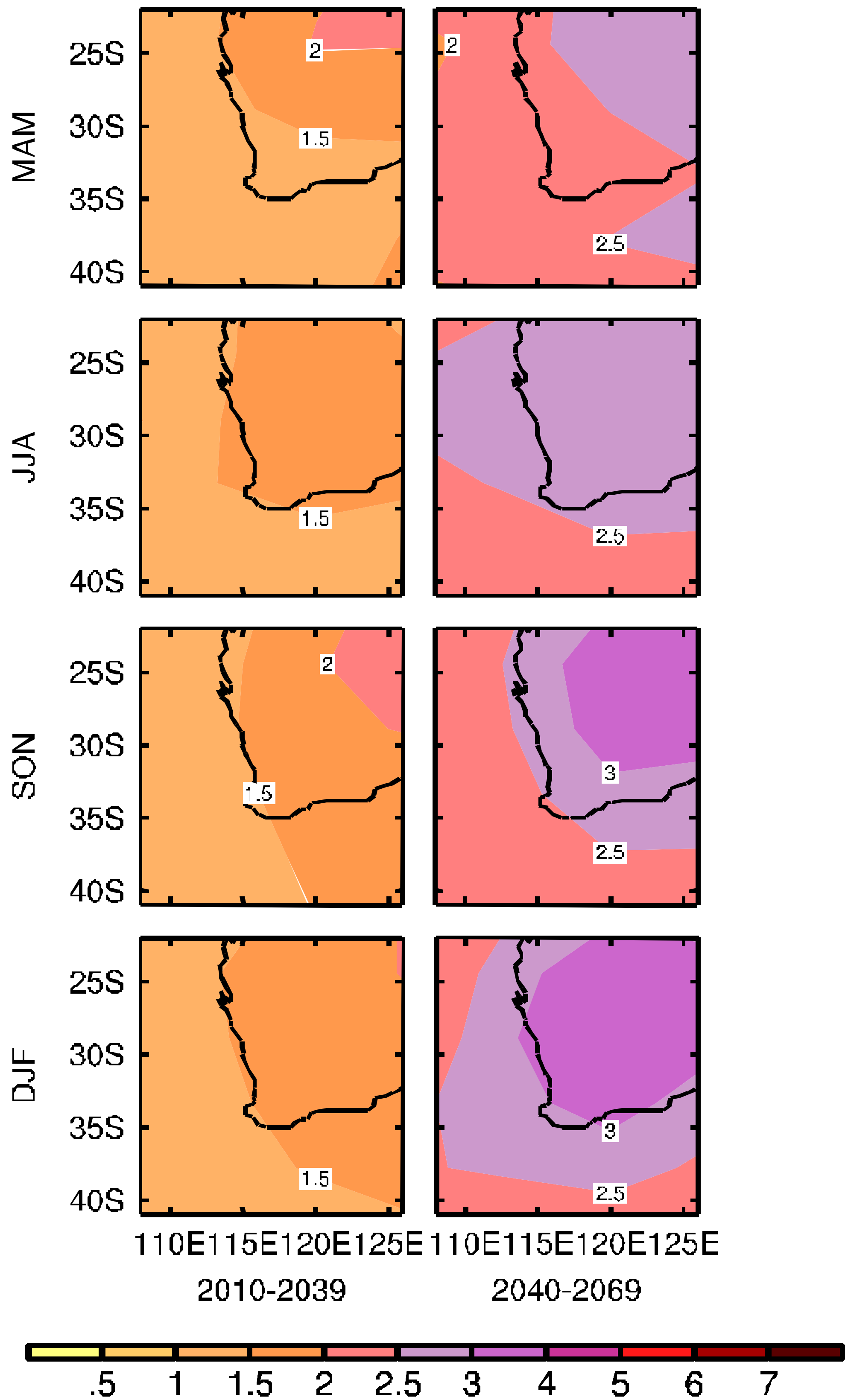

Figure 5: Non-aerosol GFDL GCM simulations of seasonal mean surface temperature change over SWA in the 2010-2039 and half of the 2040-2069 epoch. Seasons are autumn (MAM), winter (JJA), spring (SON) and summer (DJF). Surface temperature is in °C from the 1961-2000 climatology, with the colour bar on the figure showing the surface temperature contour values.

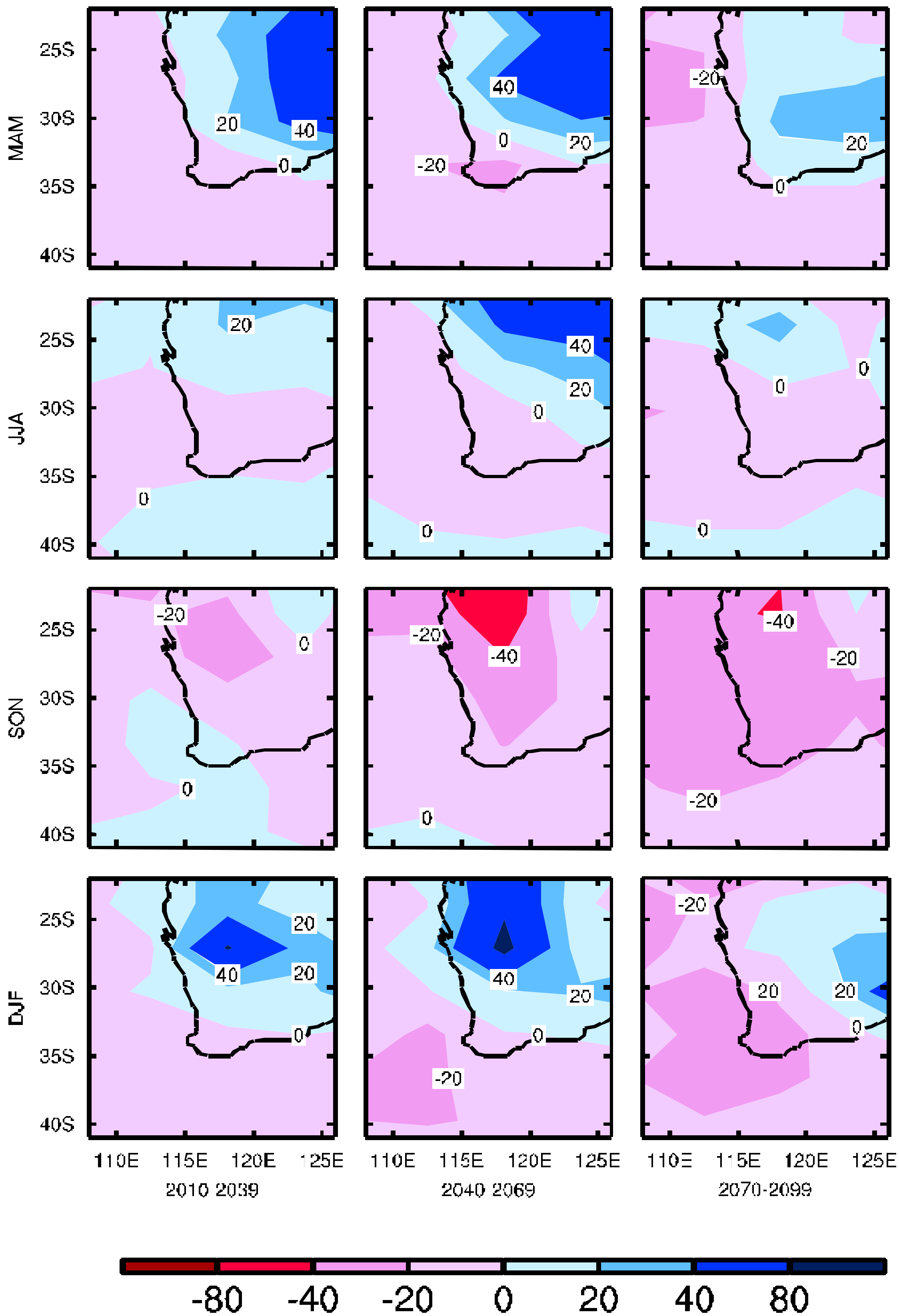

Figure 6: Non-aerosol CSIRO MARK 2 GCM simulations of percentage changes in seasonal mean rainfall over SWA in the 2010-2039, 2040-2069 and 2070-2099 epochs. Seasons are autumn (MAM), winter (JJA), spring (SON) and summer (DJF). Rainfall is in % changes from the 1961-2000 climatology, with the colour bar on the figure showing the rainfall contour values.

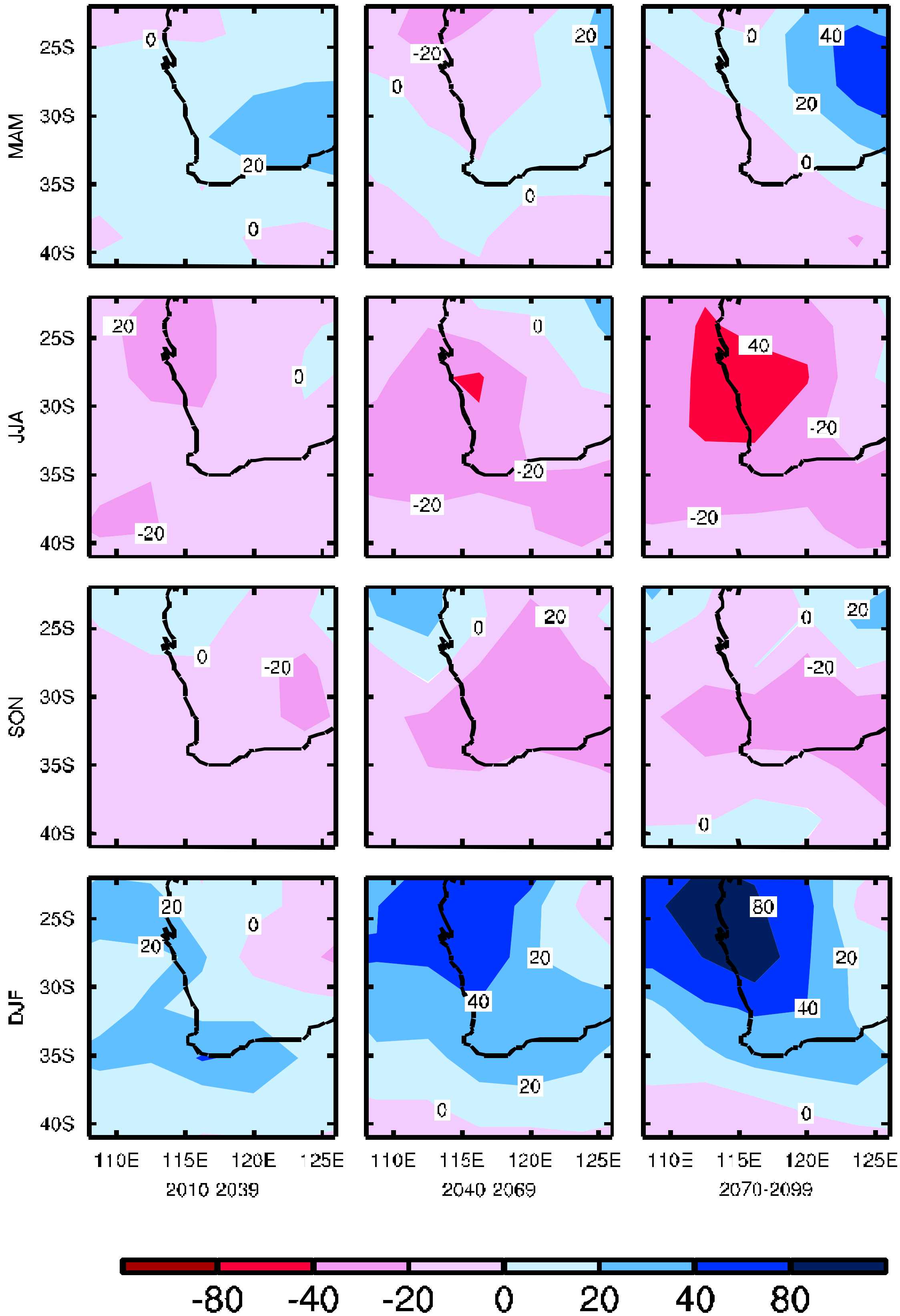

Figure 7: Non-aerosol CCC GCM simulations of percentage changes in seasonal mean rainfall over SWA in the 2010-2039, 2040-2069 and 2070-2099 epochs. Seasons are autumn (MAM), winter (JJA), spring (SON) and summer (DJF). Rainfall is in % changes from the 1961-2000 climatology, with the colour bar on the figure showing the rainfall contour values.

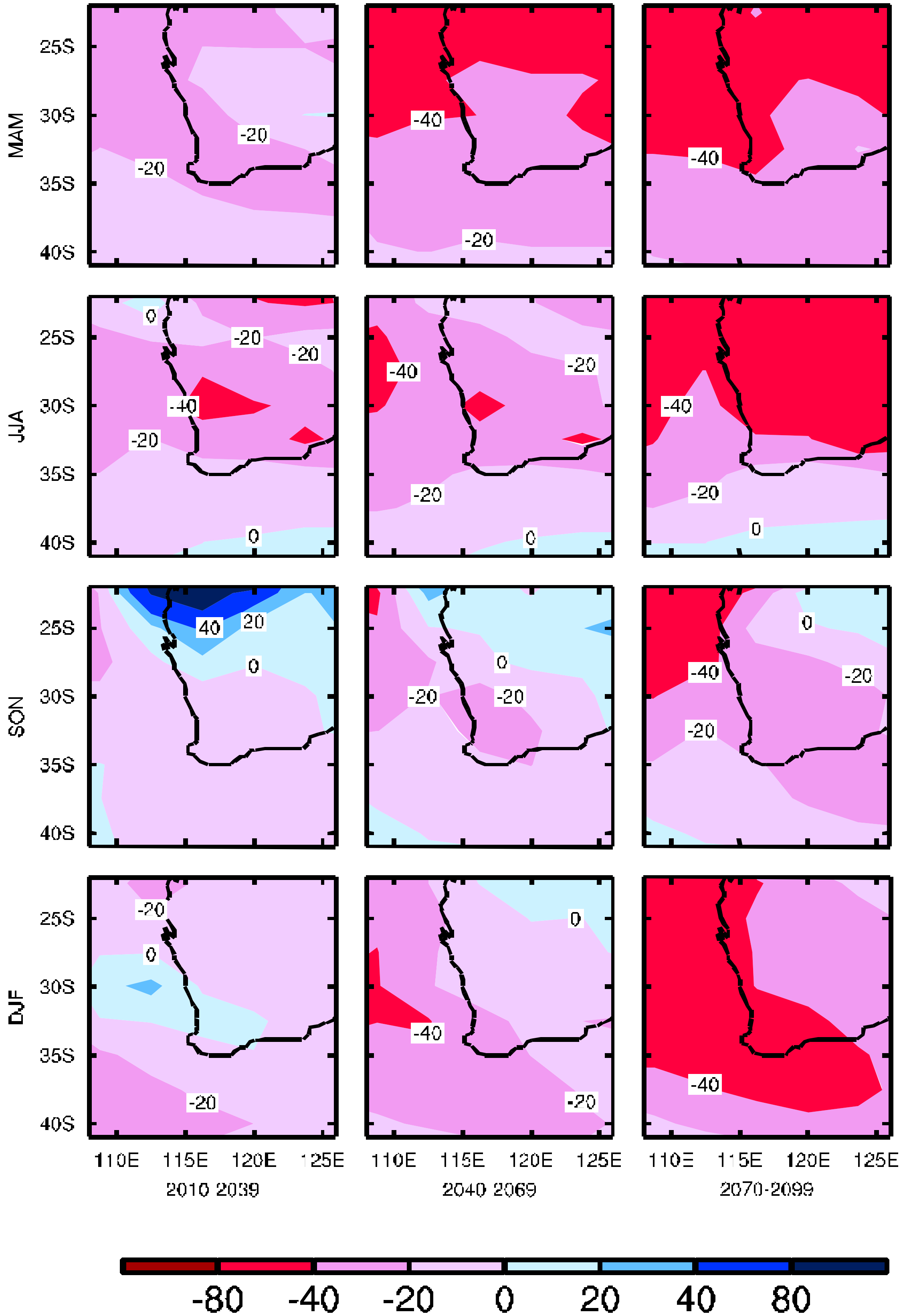

Figure 8: Non-aerosol HADCM2 GCM simulations of percentage changes in seasonal mean rainfall over SWA in the 2010-2039, 2040-2069 and 2070-2099 epochs. Seasons are autumn (MAM), winter (JJA), spring (SON) and summer (DJF). Rainfall is in % changes from the 1961-2000 climatology, with the colour bar on the figure showing the rainfall contour values.

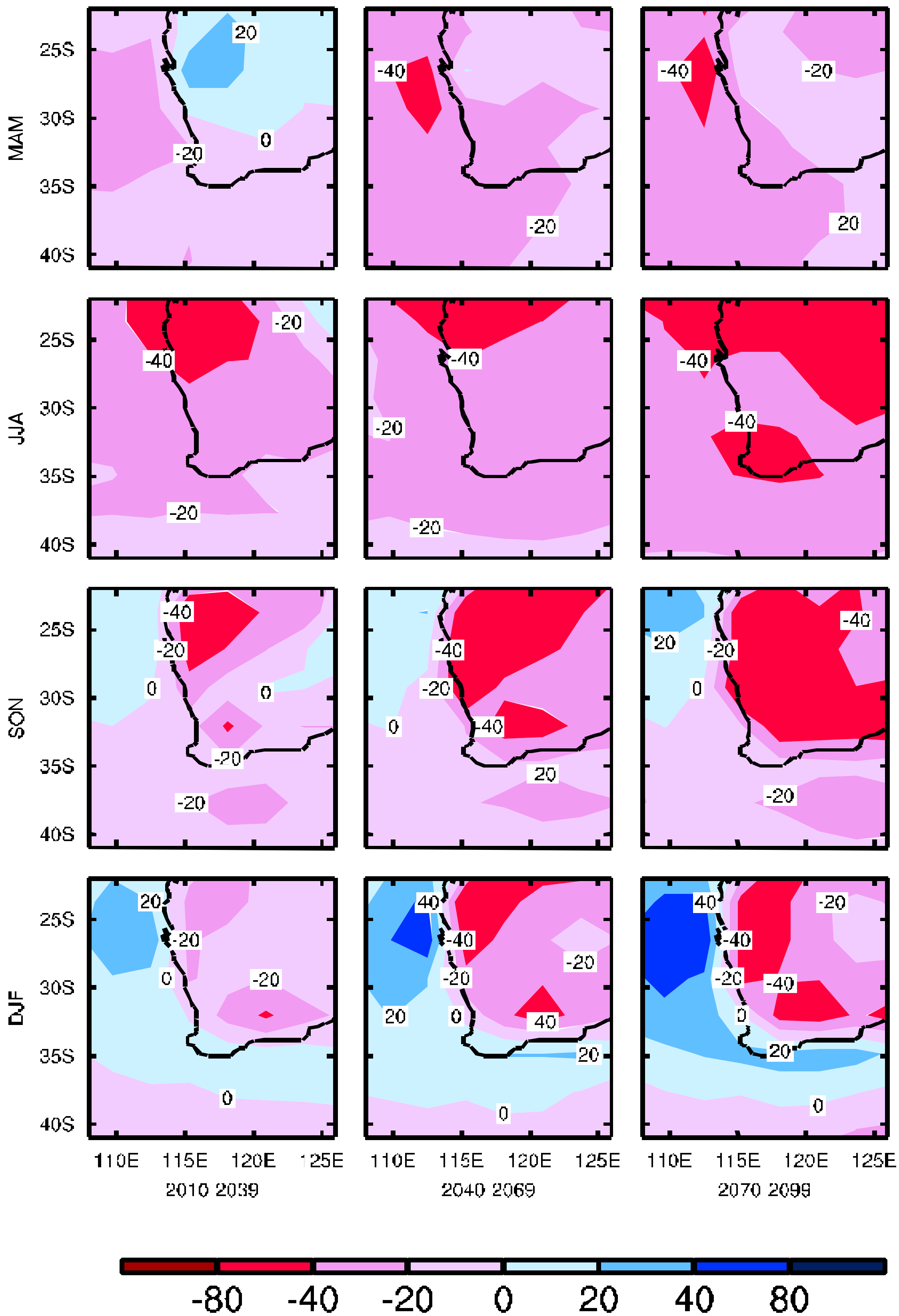

Figure 9: Non-aerosol MPI GCM simulations of percentage changes in seasonal mean rainfall over SWA in the 2010-2039, 2040-2069 and 2070-2099 epochs. Seasons are autumn (MAM), winter (JJA), spring (SON) and summer (DJF). Rainfall is in % changes from the 1961-2000 climatology, with the colour bar on the figure showing the rainfall contour values.

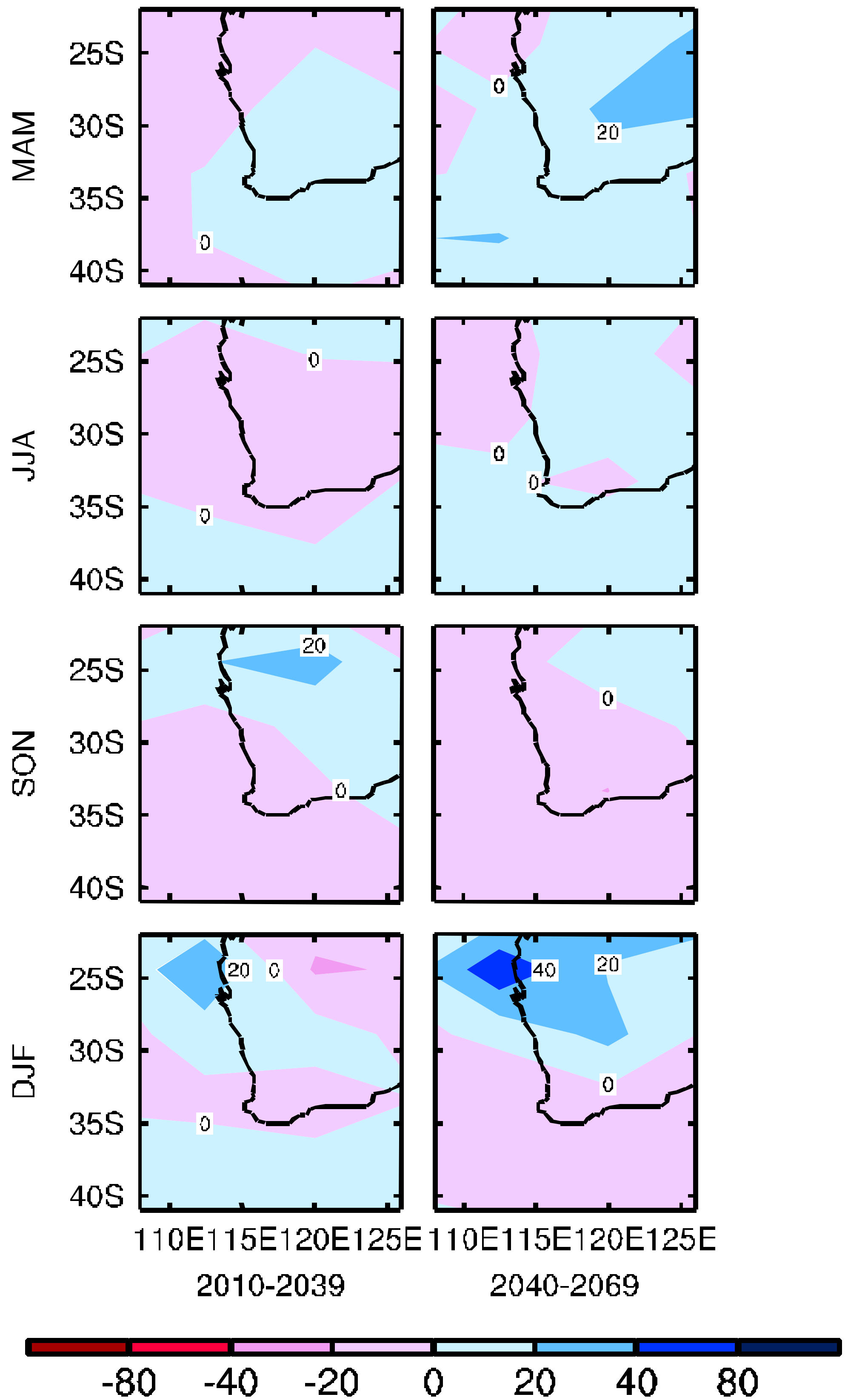

Figure 10: Non-aerosol GFDL GCM simulations of percentage changes in seasonal mean rainfall over SWA in the 2010-2039 and half of the 2040-2069 epoch. Seasons are autumn (MAM), winter (JJA), spring (SON) and summer (DJF). Rainfall is in % changes from the 1961-2000 climatology, with the colour bar on the figure showing the rainfall contour values.

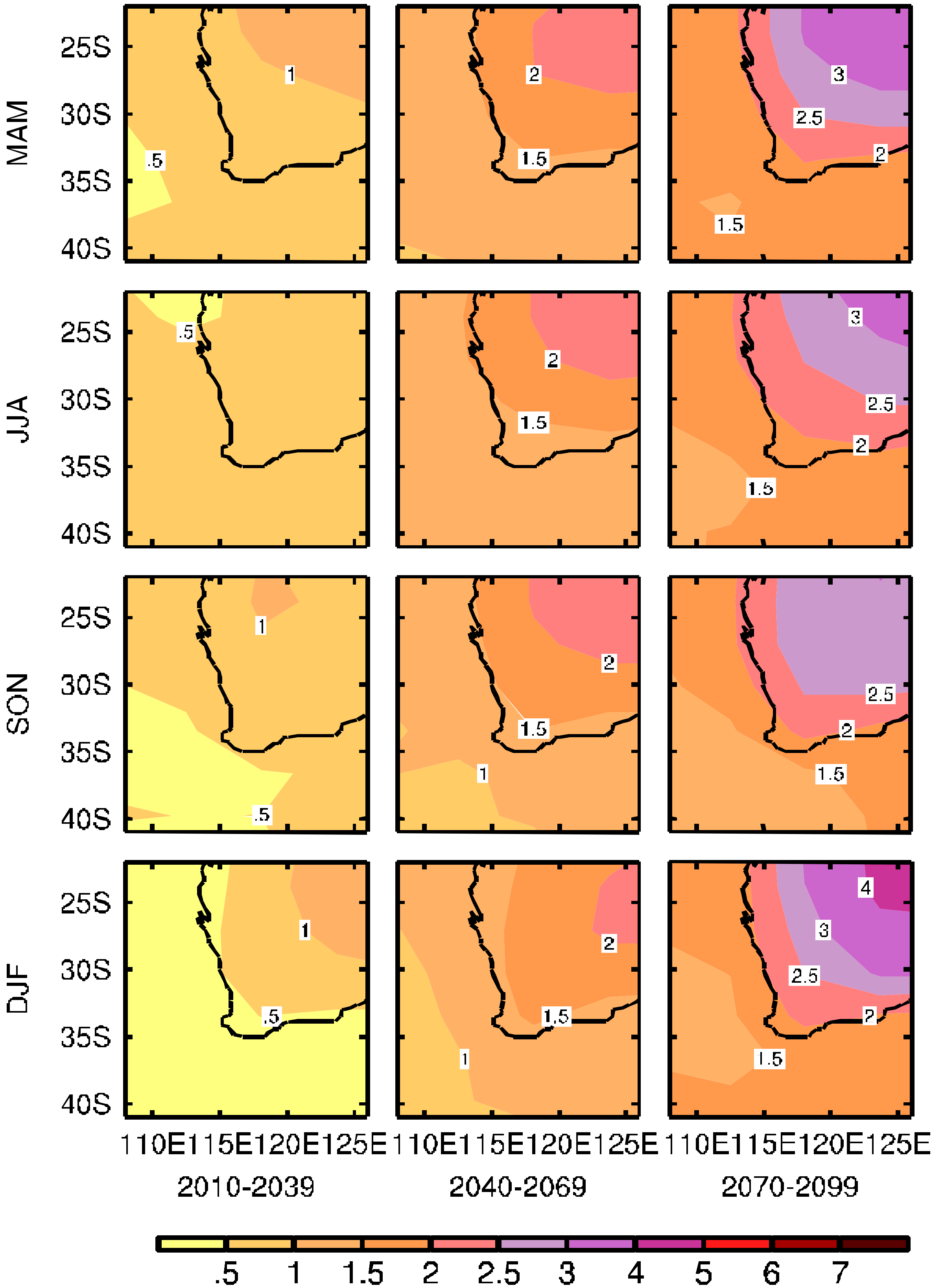

Figure 11: Aerosol CSIRO MARK 2 GCM simulations of seasonal mean surface temperature change over SWA in the 2010-2039, 2040-2069 and 2070-2099 epochs. Seasons are autumn (MAM), winter (JJA), spring (SON) and summer (DJF). Surface temperature is in °C, with the colour bar on the figure showing the surface temperature contour values.

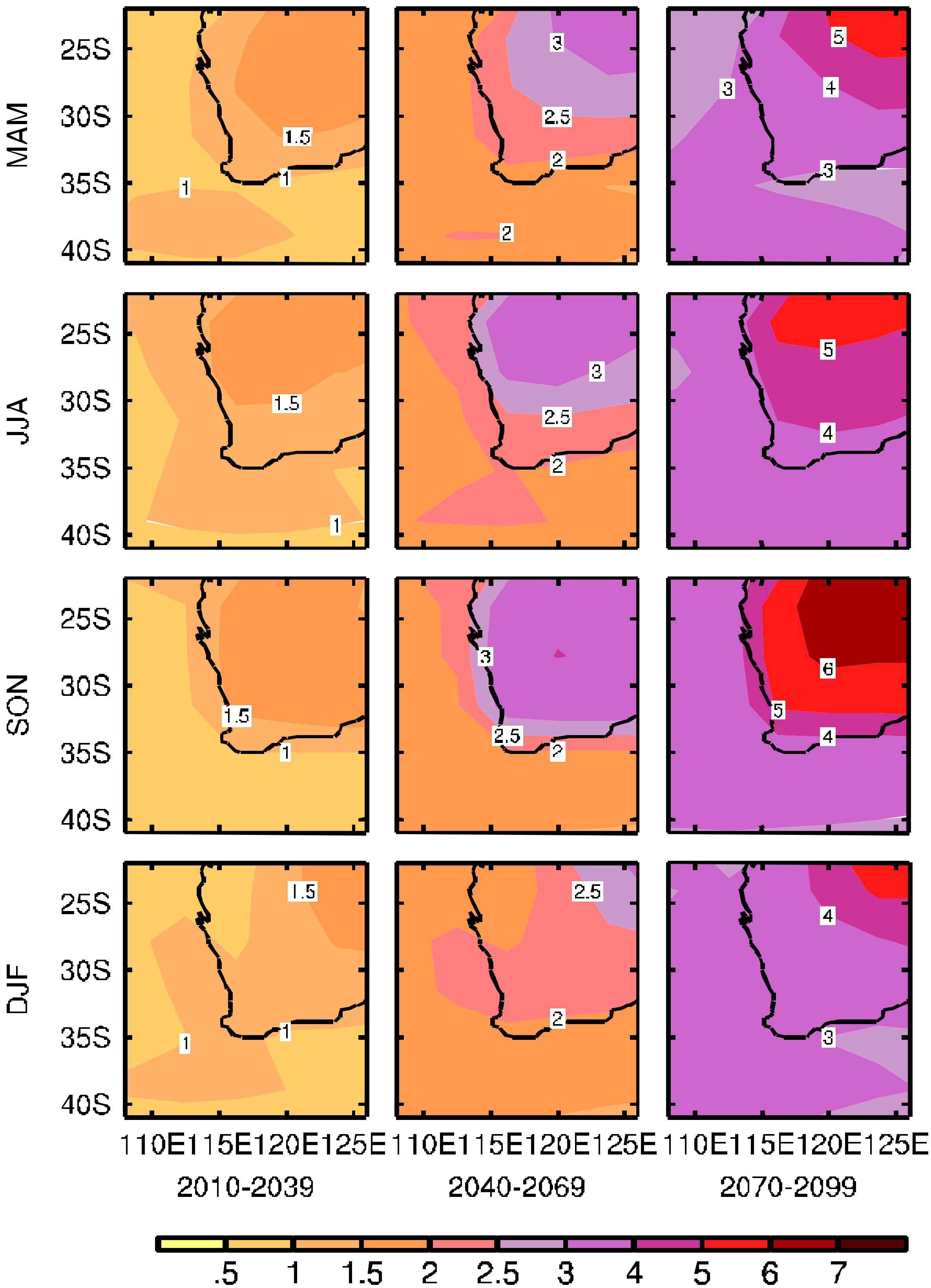

Figure 12: Aerosol CCC GCM simulations of seasonal mean surface temperature change over SWA in the 2010-2039, 2040-2069 and 2070-2099 epochs. Seasons are autumn (MAM), winter (JJA), spring (SON) and summer (DJF). Surface temperature is in °C, with the colour bar on the figure showing the surface temperature contour values.

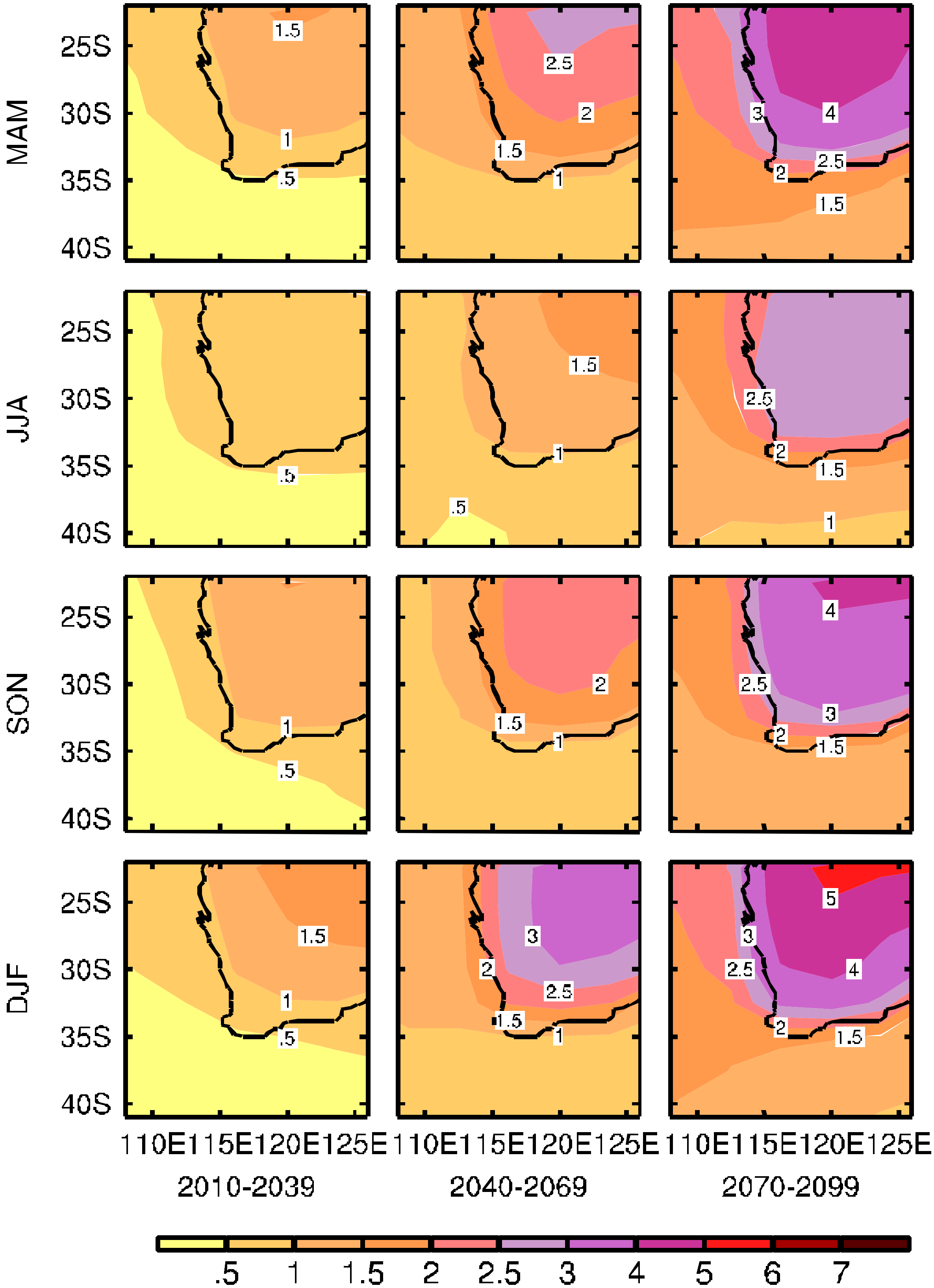

Figure 13: Aerosol HADCM2 GCM simulations of seasonal mean surface temperature change over SWA in the 2010-2039, 2040-2069 and 2070-2099 epochs. Seasons are autumn (MAM), winter (JJA), spring (SON) and summer (DJF). Surface temperature is in °C, with the colour bar on the figure showing the surface temperature contour values.

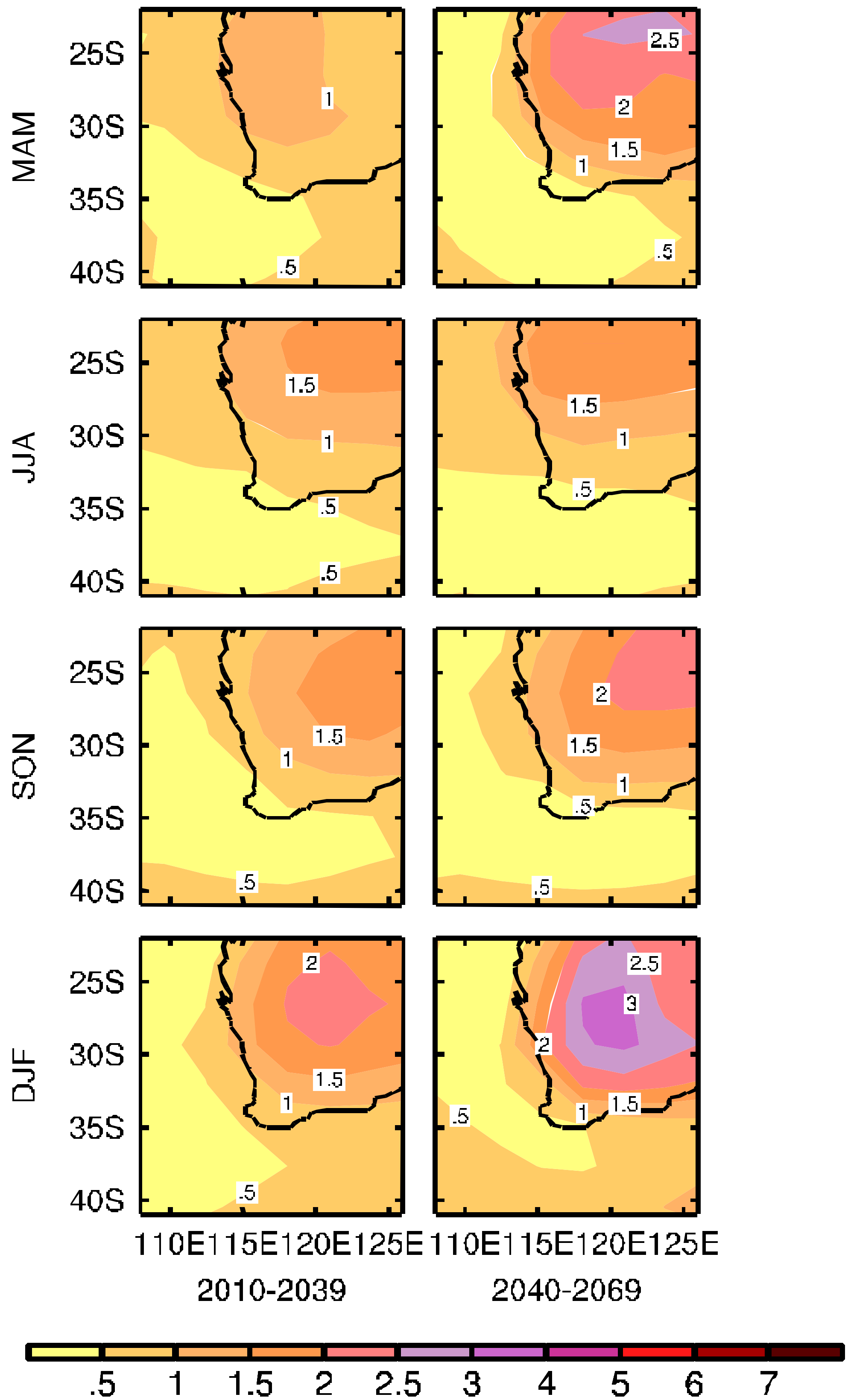

Figure 14: Aerosol MPI GCM simulations of seasonal mean surface temperature change over SWA in the 2010-2039 and half of the 2040-2069 epoch. Seasons are autumn (MAM), winter (JJA), spring (SON) and summer (DJF). Surface temperature is in °C, with the colour bar on the figure showing the surface temperature contour values.

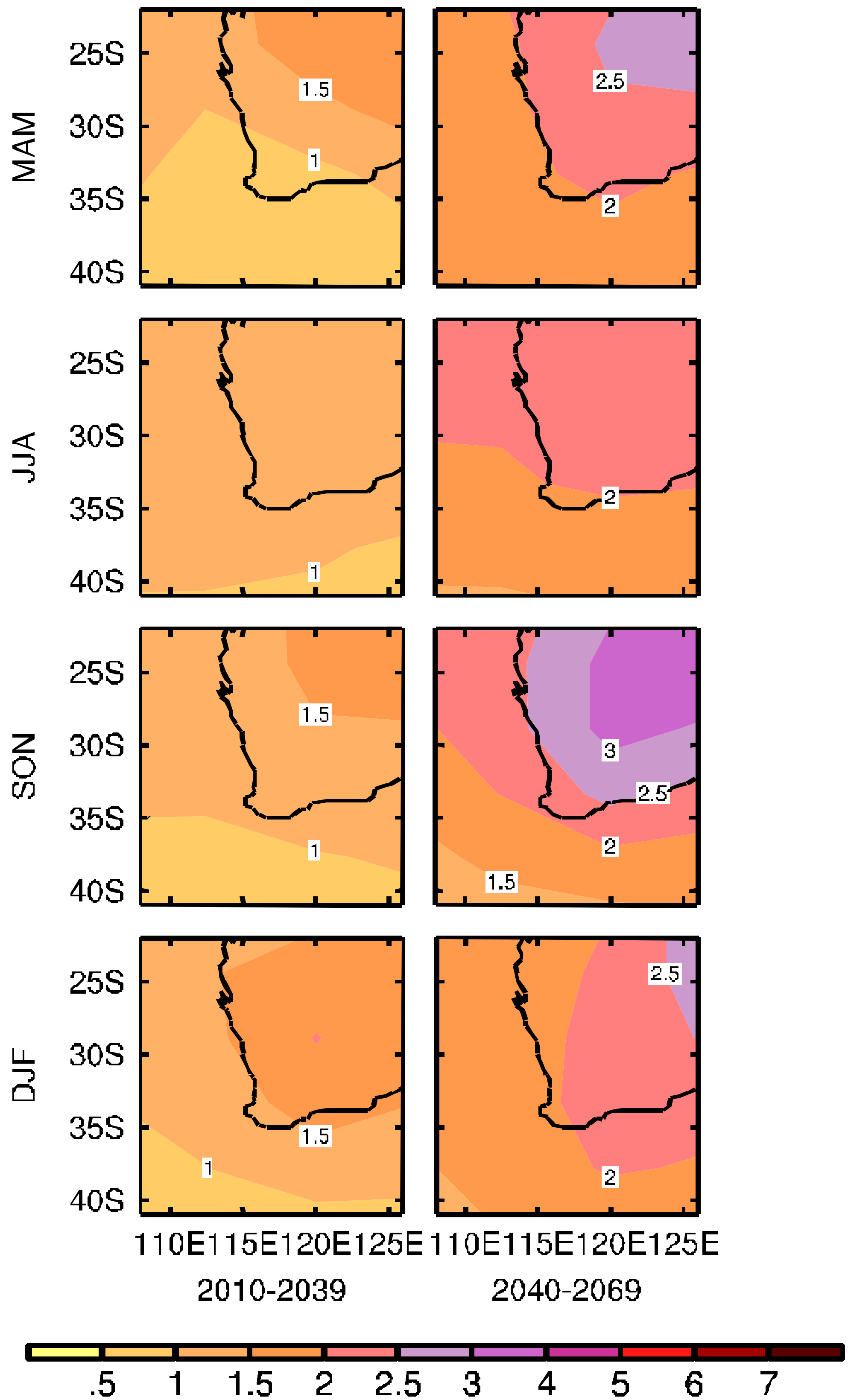

Figure 15: Aerosol GFDL GCM simulations of seasonal mean surface temperature change over SWA in the 2010-2039 and half of the 2040-2069 epoch. Seasons are autumn (MAM), winter (JJA), spring (SON) and summer (DJF). Surface temperature is in °C, with the colour bar on the figure showing the surface temperature contour values.

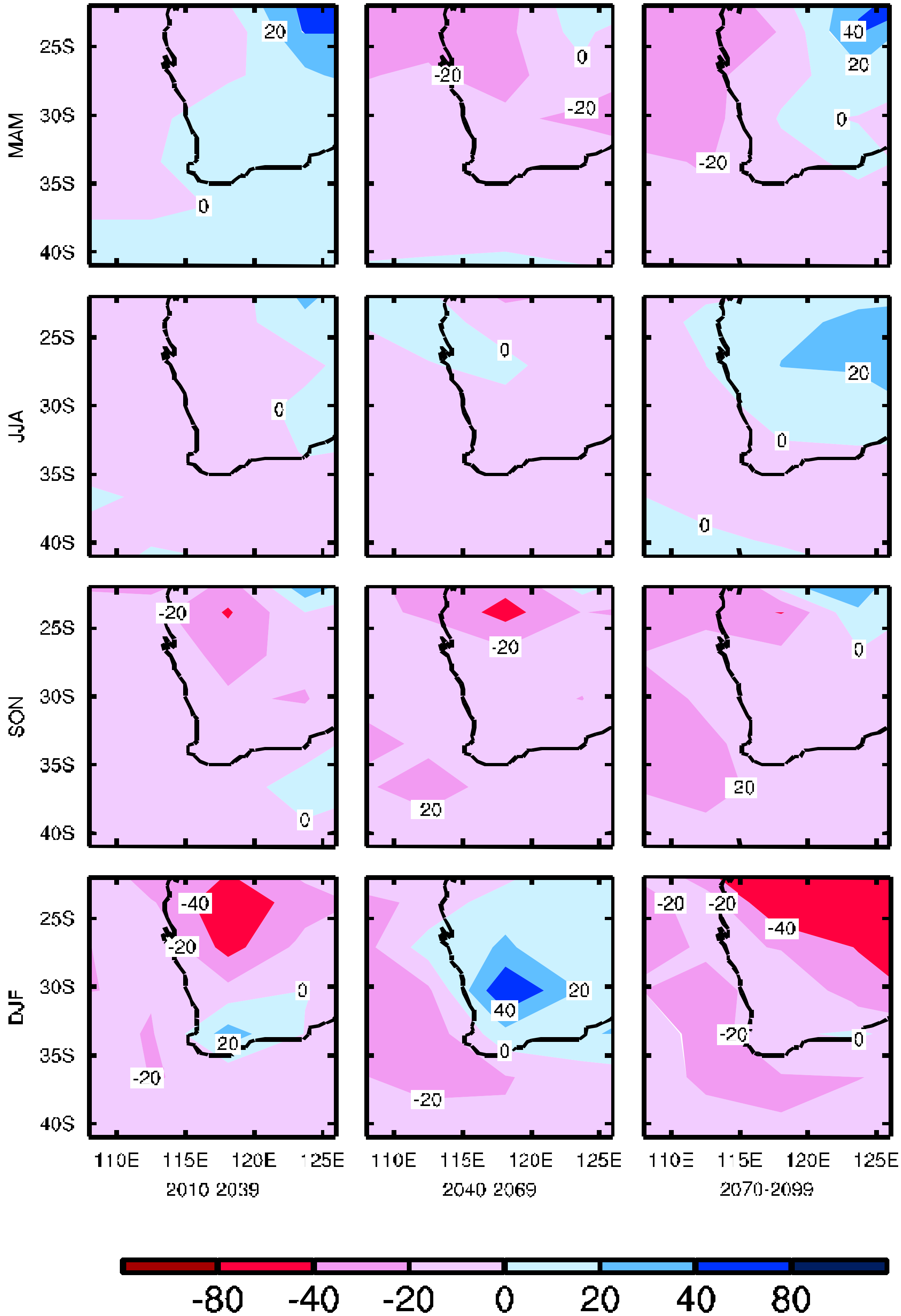

Figure 16: Aerosol CSIRO MARK 2 GCM simulations of percentage changes in seasonal mean rainfall over SWA in the 2010-2039, 2040-2069 and 2070-2099 epochs. Seasons are autumn (MAM), winter (JJA), spring (SON) and summer (DJF). Rainfall is in % changes from the 1961-2000 climatology, with the colour bar on the figure showing the rainfall contour values.

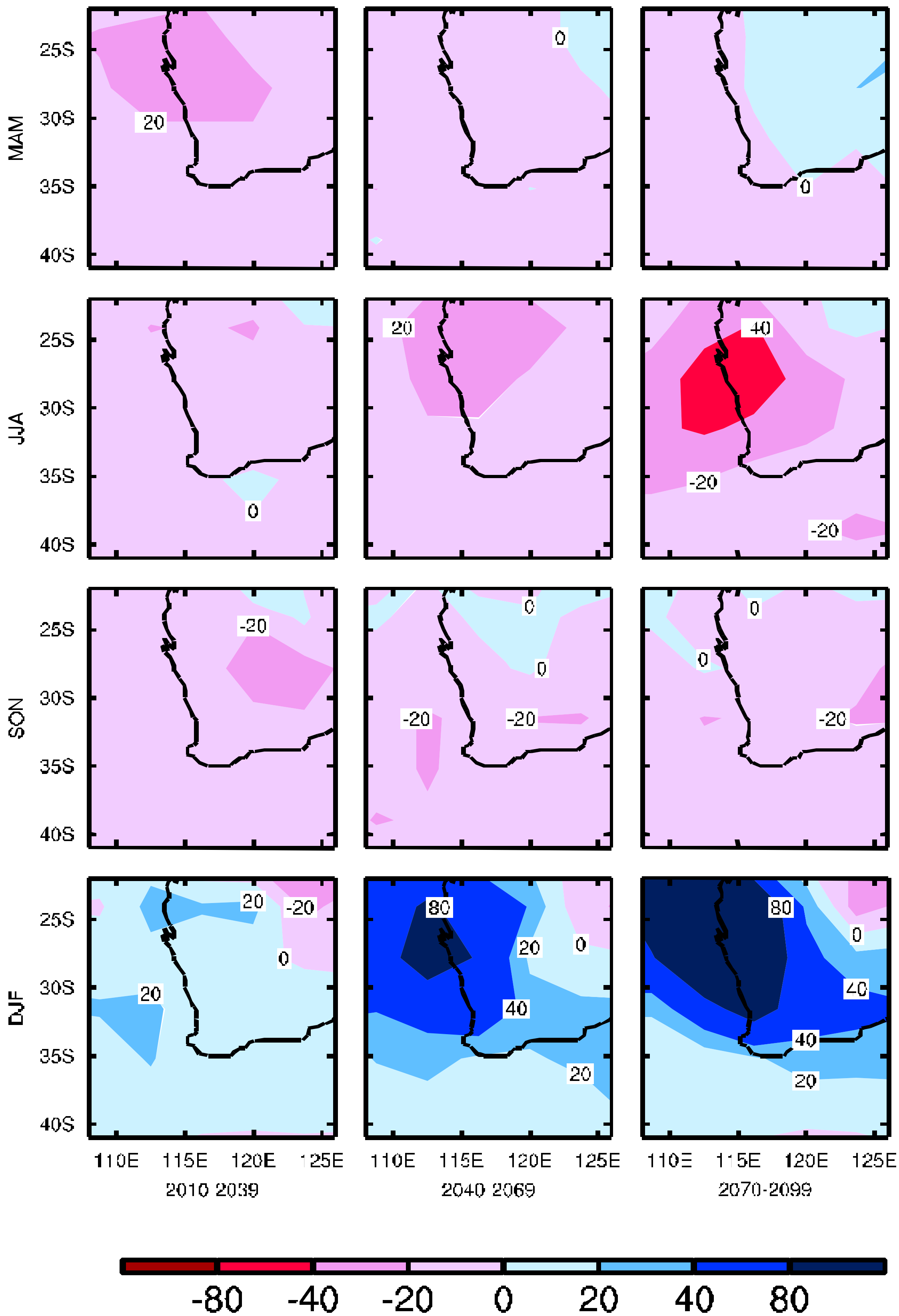

Figure 17: Aerosol CCC GCM simulations of percentage changes in seasonal mean rainfall over SWA in the 2010-2039, 2040-2069 and 2070-2099 epochs. Seasons are autumn (MAM), winter (JJA), spring (SON) and summer (DJF). Rainfall is in % changes from the 1961-2000 climatology, with the colour bar on the figure showing the rainfall contour values.

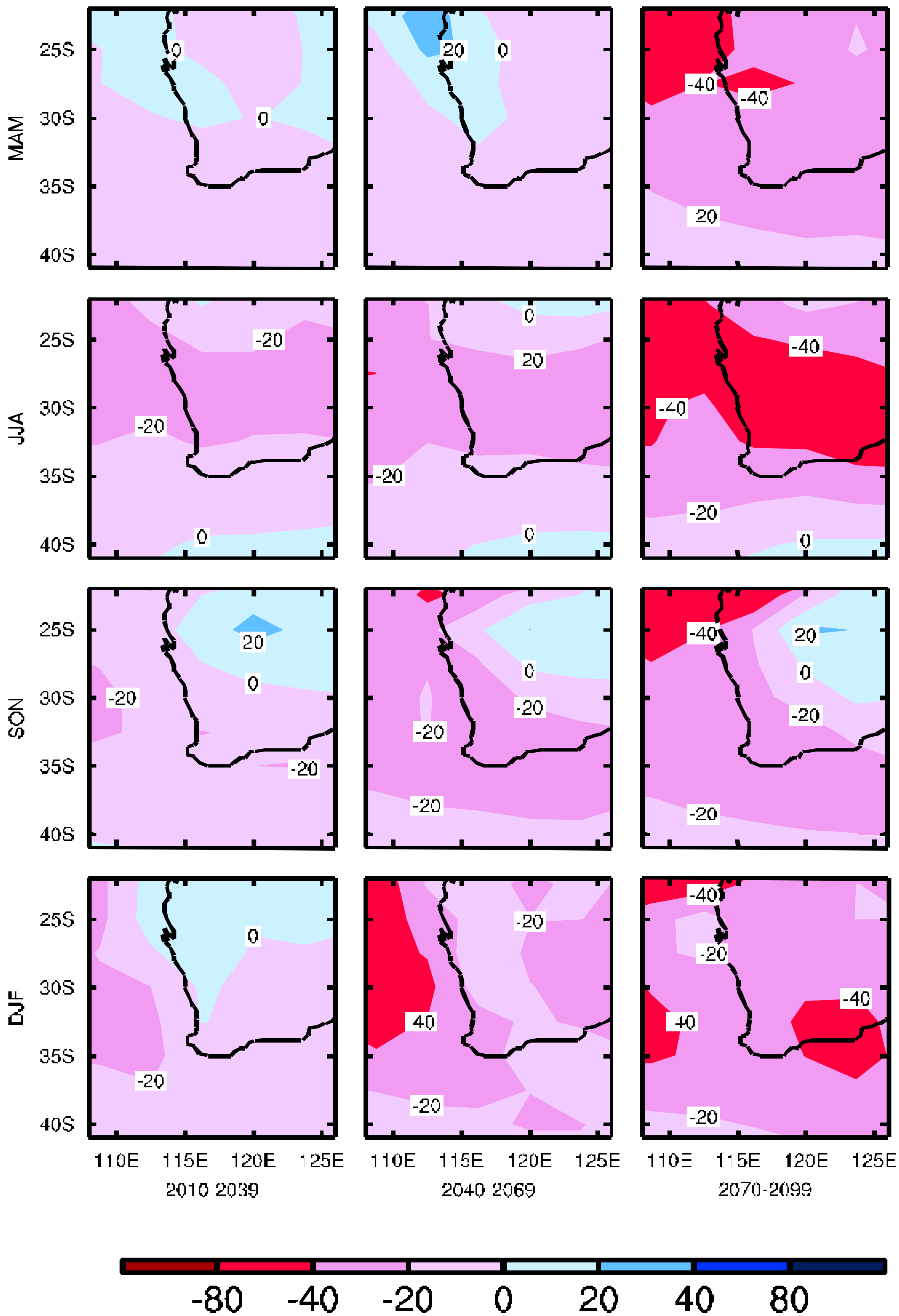

Figure 18: Aerosol HADCM2 GCM simulations of percentage changes in seasonal mean rainfall over SWA in the 2010-2039, 2040-2069 and 2070-2099 epochs. Seasons are autumn (MAM), winter (JJA), spring (SON) and summer (DJF). Rainfall is in % changes from the 1961-2000 climatology, with the colour bar on the figure showing the rainfall contour values.

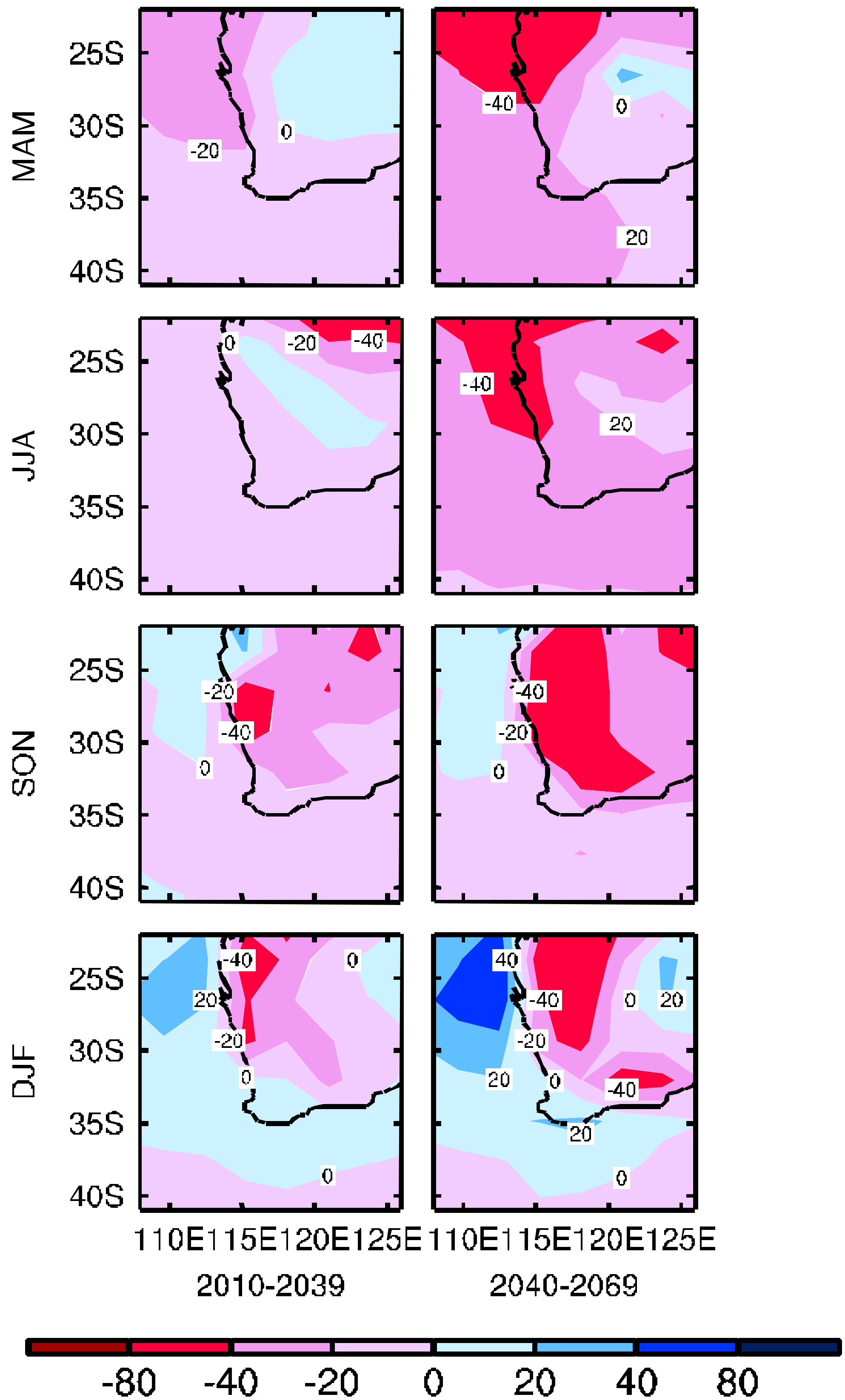

Figure 19: Aerosol MPI GCM simulations of percentage changes in seasonal mean rainfall over SWA in the 2010-2039 and half of the 2040-2069 epoch. Seasons are autumn (MAM), winter (JJA), spring (SON) and summer (DJF). Rainfall is in % changes from the 1961-2000 climatology, with the colour bar on the figure showing the rainfall contour values.

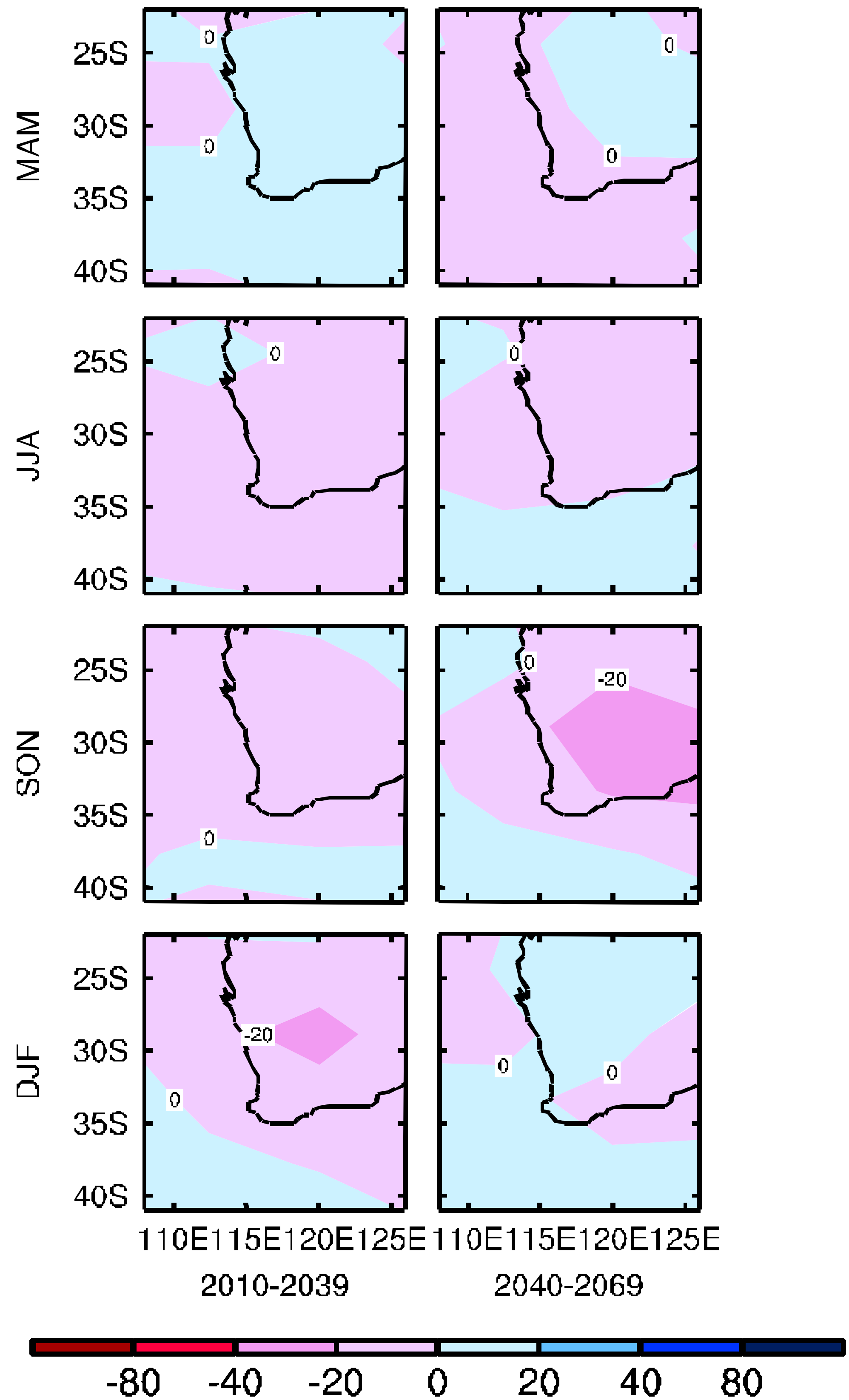

Figure 20: Aerosol GFDL GCM simulations of percentage changes in seasonal mean rainfall over SWA in the 2010-2039 and half of the 2040-2069 epoch. Seasons are autumn (MAM), winter (JJA), spring (SON) and summer (DJF). Rainfall is in % changes from the 1961-2000 climatology, with the colour bar on the figure showing the rainfall contour values.

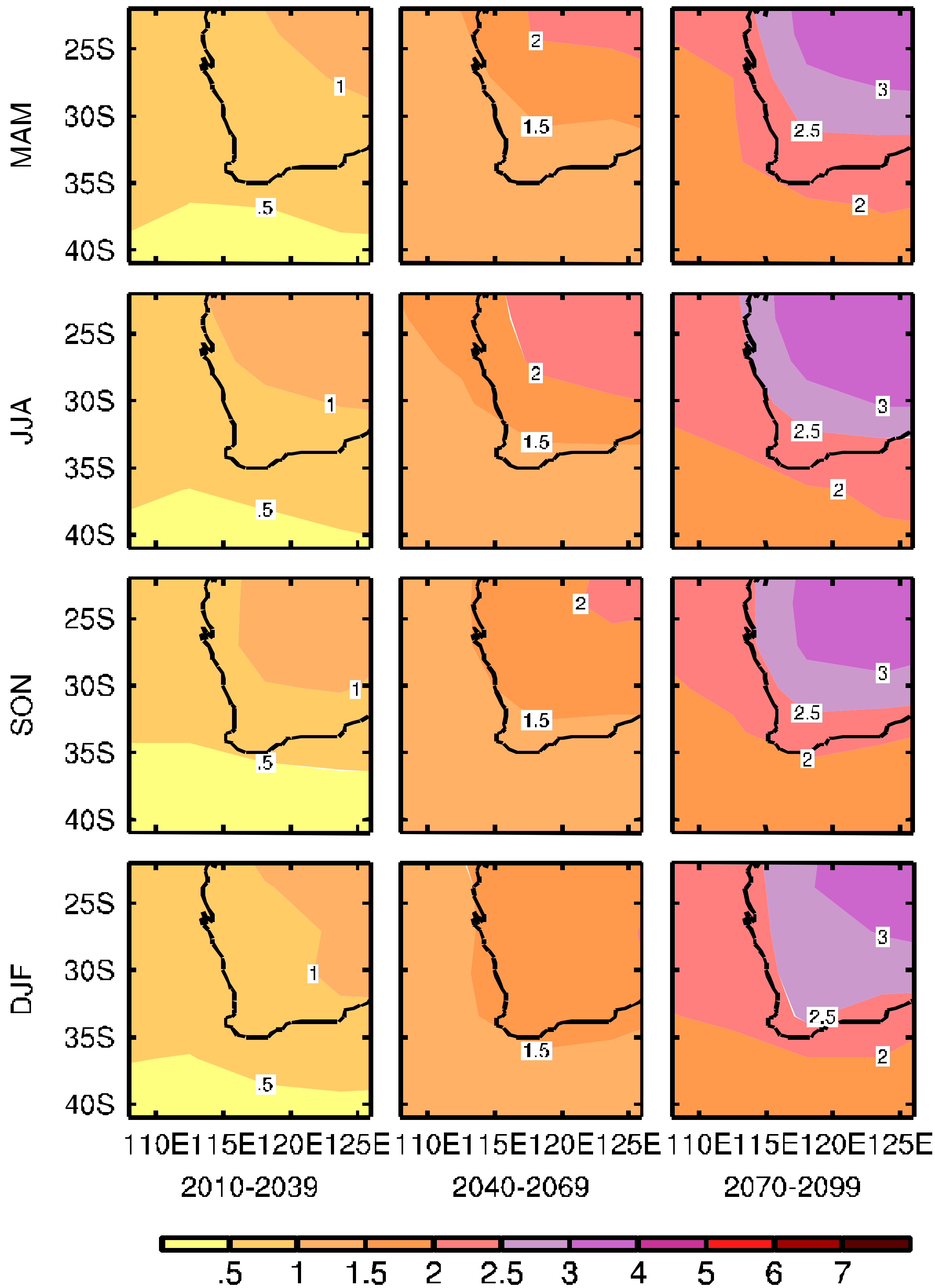

Figure 22: Non-aerosol CSIRO MARK 2 GCM BAU simulations of seasonal mean surface temperature change over SWA in the 2010-2039, 2040-2069 and 2070-2099 epochs. Seasons are autumn (MAM), winter (JJA), spring (SON) and summer (DJF). Surface temperature is in °C, with the colour bar on the figure showing the surface temperature contour values.

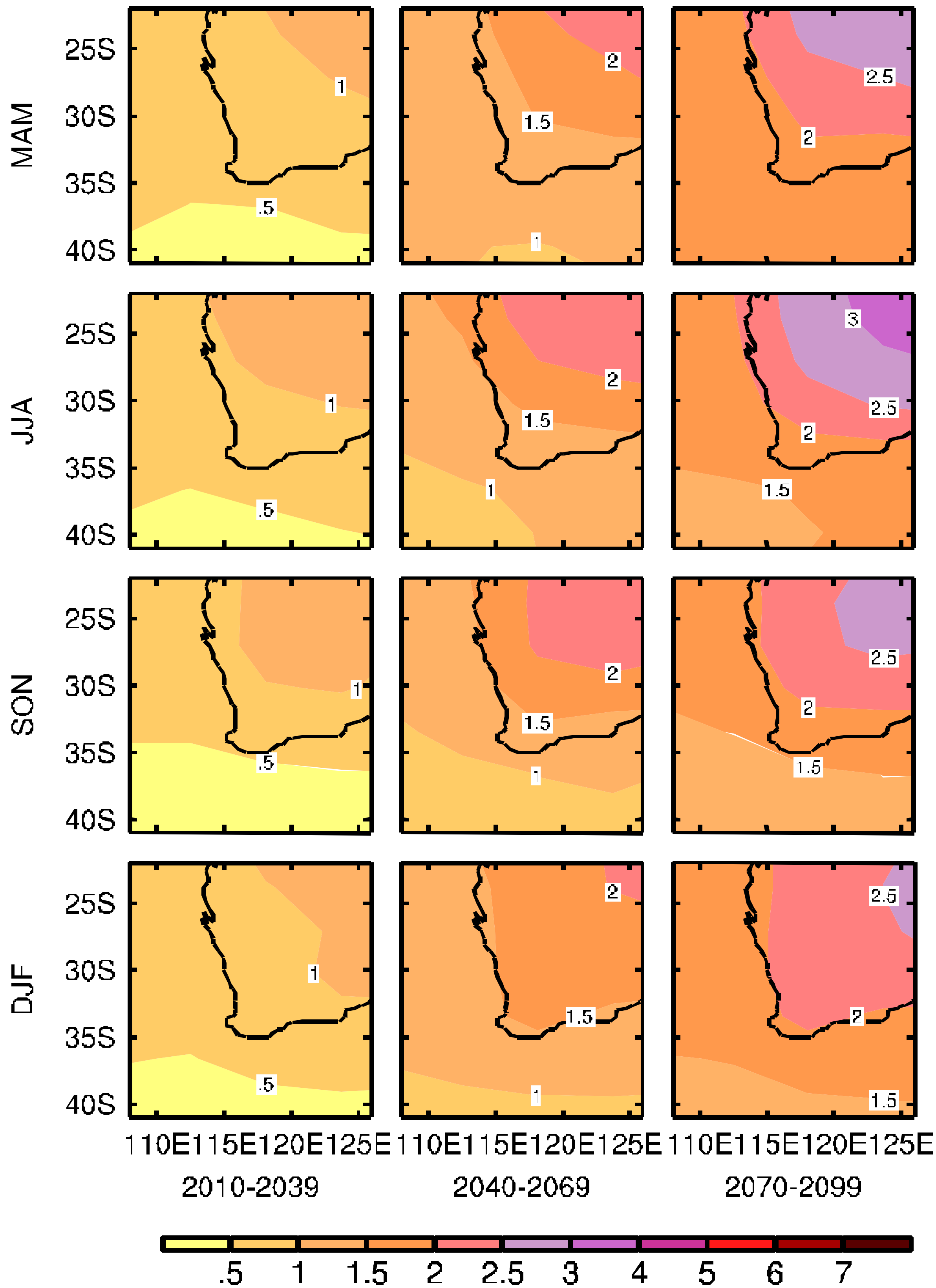

Figure 23: Non-aerosol CSIRO MARK 2 GCM PL simulations of seasonal mean surface temperature change over SWA in the 2010-2039, 2040-2069 and 2070-2099 epochs. Seasons are autumn (MAM), winter (JJA), spring (SON) and summer (DJF). Surface temperature is in °C, with the colour bar on the figure showing the surface temperature contour values.

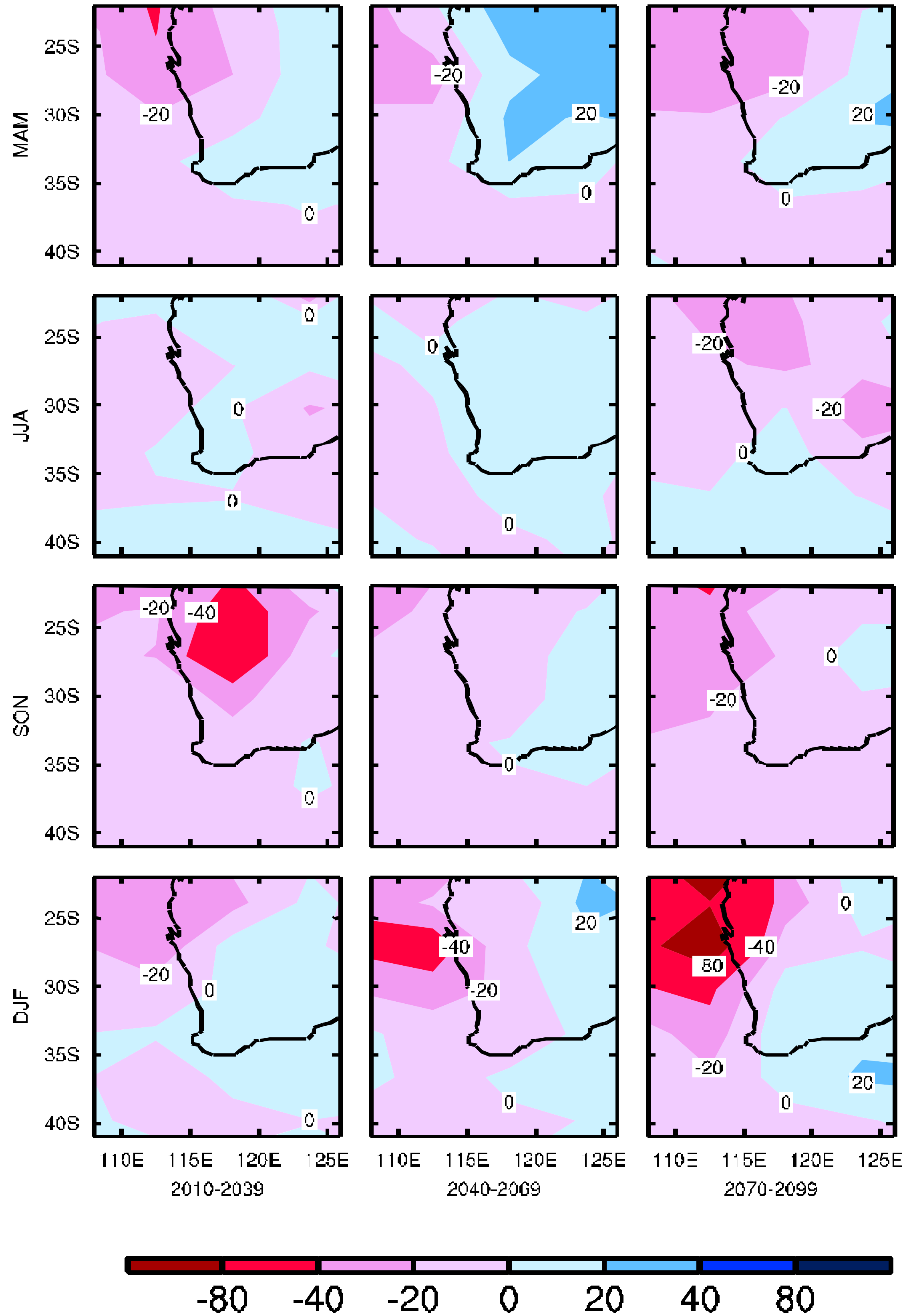

Figure 24: Non-aerosol CSIRO MARK 2 GCM BAU simulations of percentage changes in seasonal mean rainfall over SWA in the 2010-2039, 2040-2069 and 2070-2099 epochs. Seasons are autumn (MAM), winter (JJA), spring (SON) and summer (DJF). Rainfall is in % changes from the 1961-2000 climatology, with the colour bar on the figure showing the rainfall contour values.

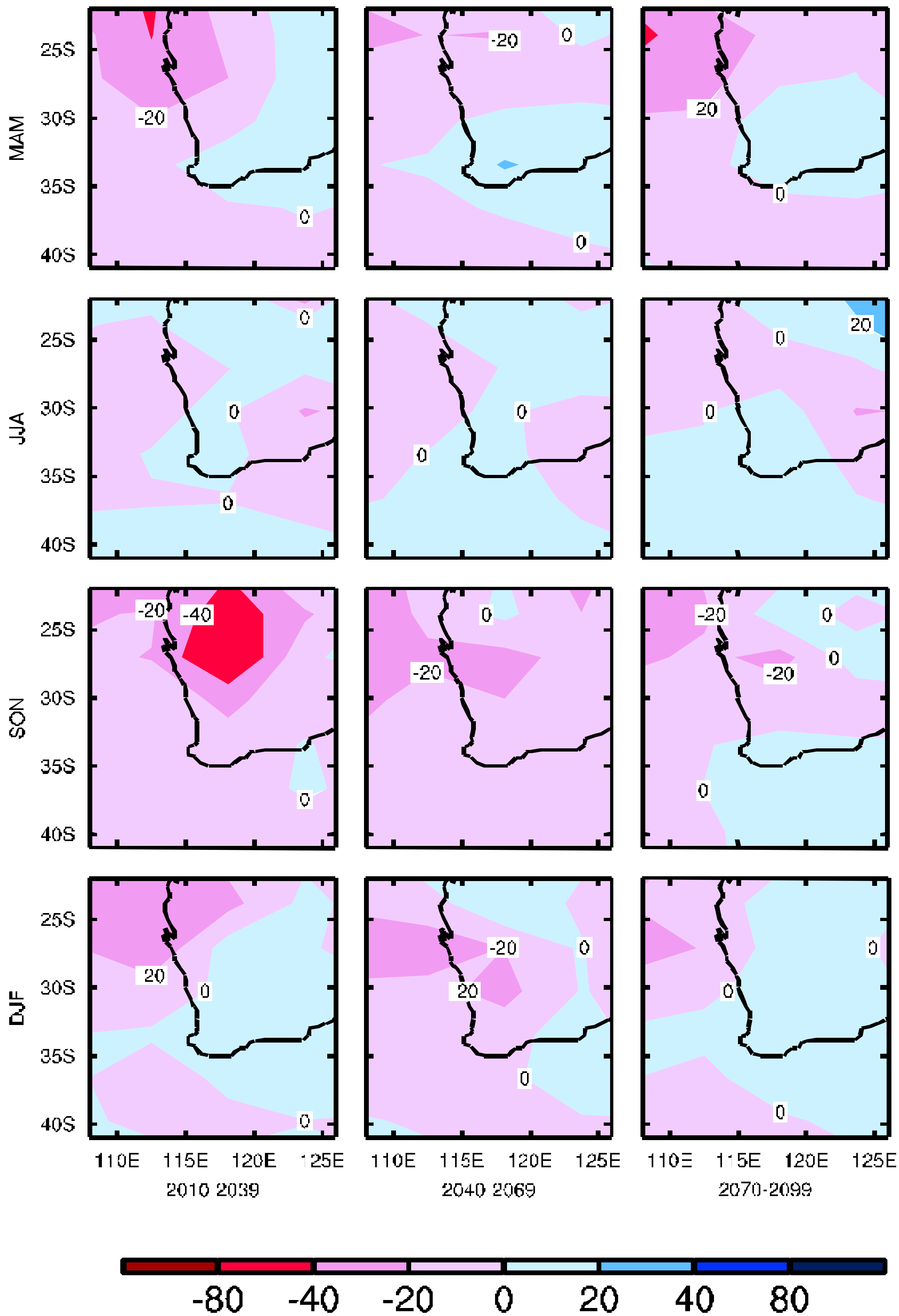

Figure 25: Non-aerosol CSIRO MARK 2 GCM PL simulations of percentage changes in seasonal mean rainfall over SWA in the 2010-2039, 2040-2069 and 2070-2099 epochs. Seasons are autumn (MAM), winter (JJA), spring (SON) and summer (DJF). Rainfall is in % changes from the 1961-2000 climatology, with the colour bar on the figure showing the rainfall contour values.

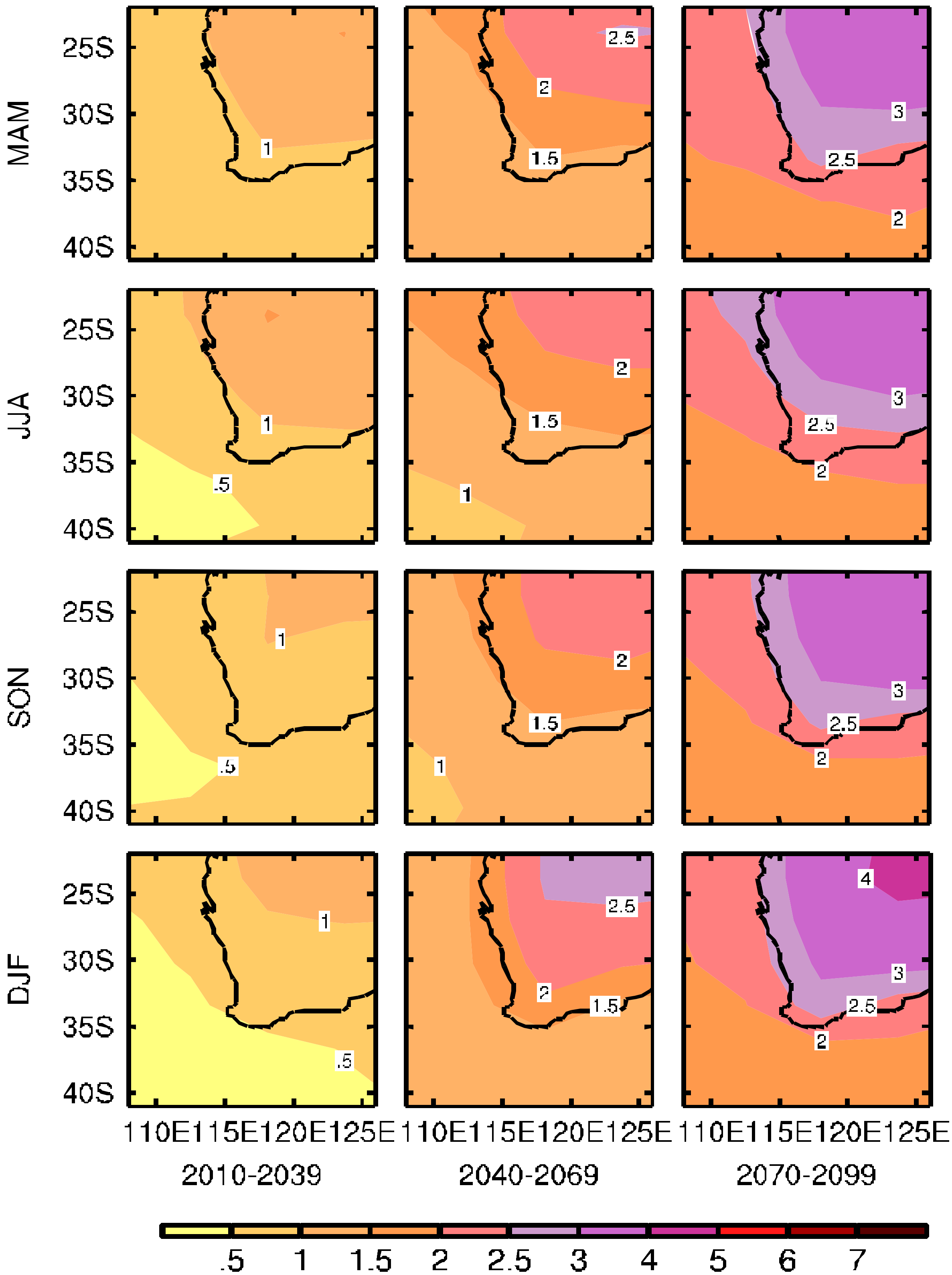

Figure 26: Aerosol CSIRO MARK 2 GCM BAU simulations of seasonal mean surface temperature change over SWA in the 2010-2039, 2040-2069 and 2070-2099 epochs. Seasons are autumn (MAM), winter (JJA), spring (SON) and summer (DJF). Surface temperature is in °C, with the colour bar on the figure showing the surface temperature contour values.

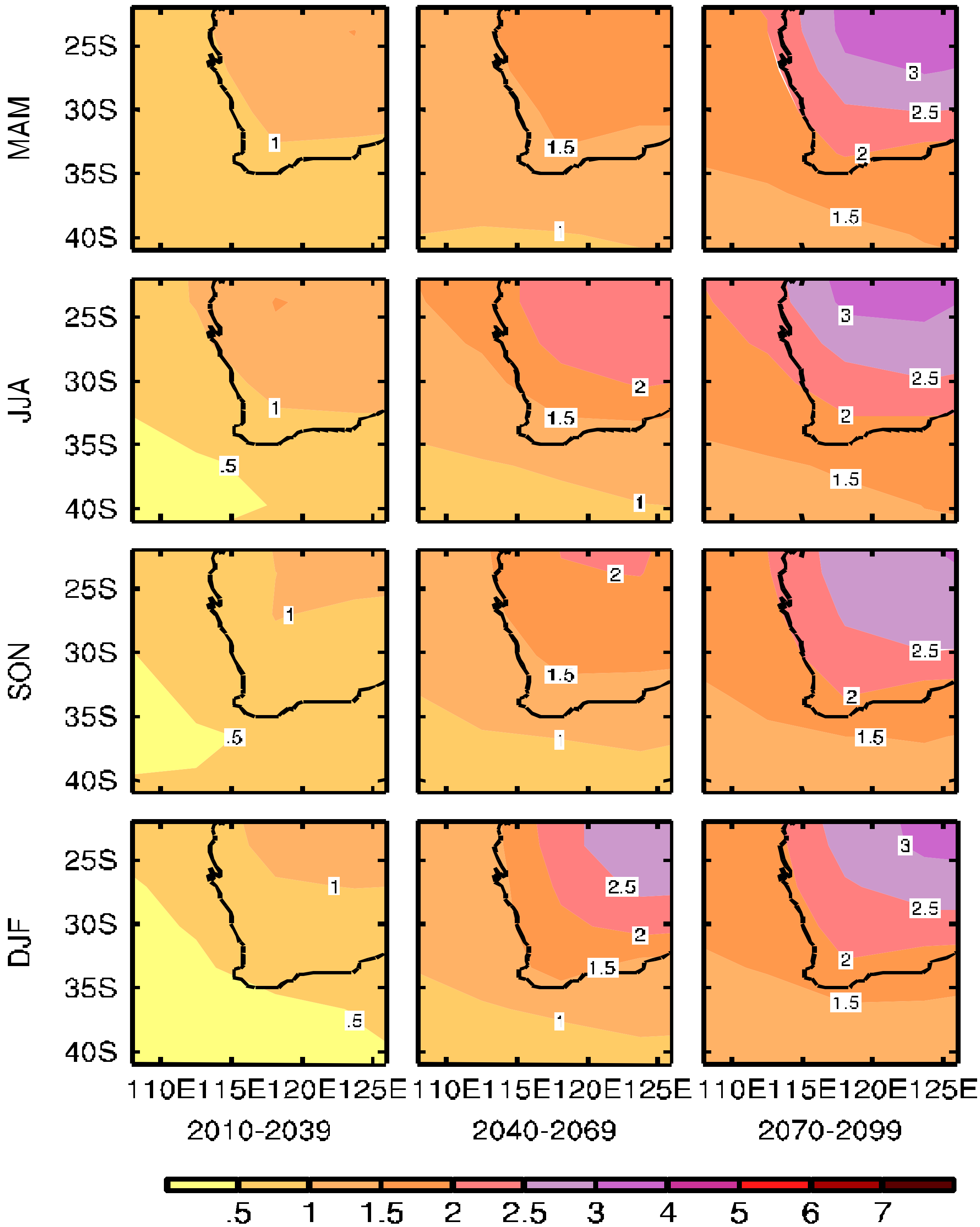

Figure 27: Aerosol CSIRO MARK 2 GCM PL simulations of seasonal mean surface temperature change over SWA in the 2010-2039, 2040-2069 and 2070-2099 epochs. Seasons are autumn (MAM), winter (JJA), spring (SON) and summer (DJF). Surface temperature is in °C, with the colour bar on the figure showing the surface temperature contour values.

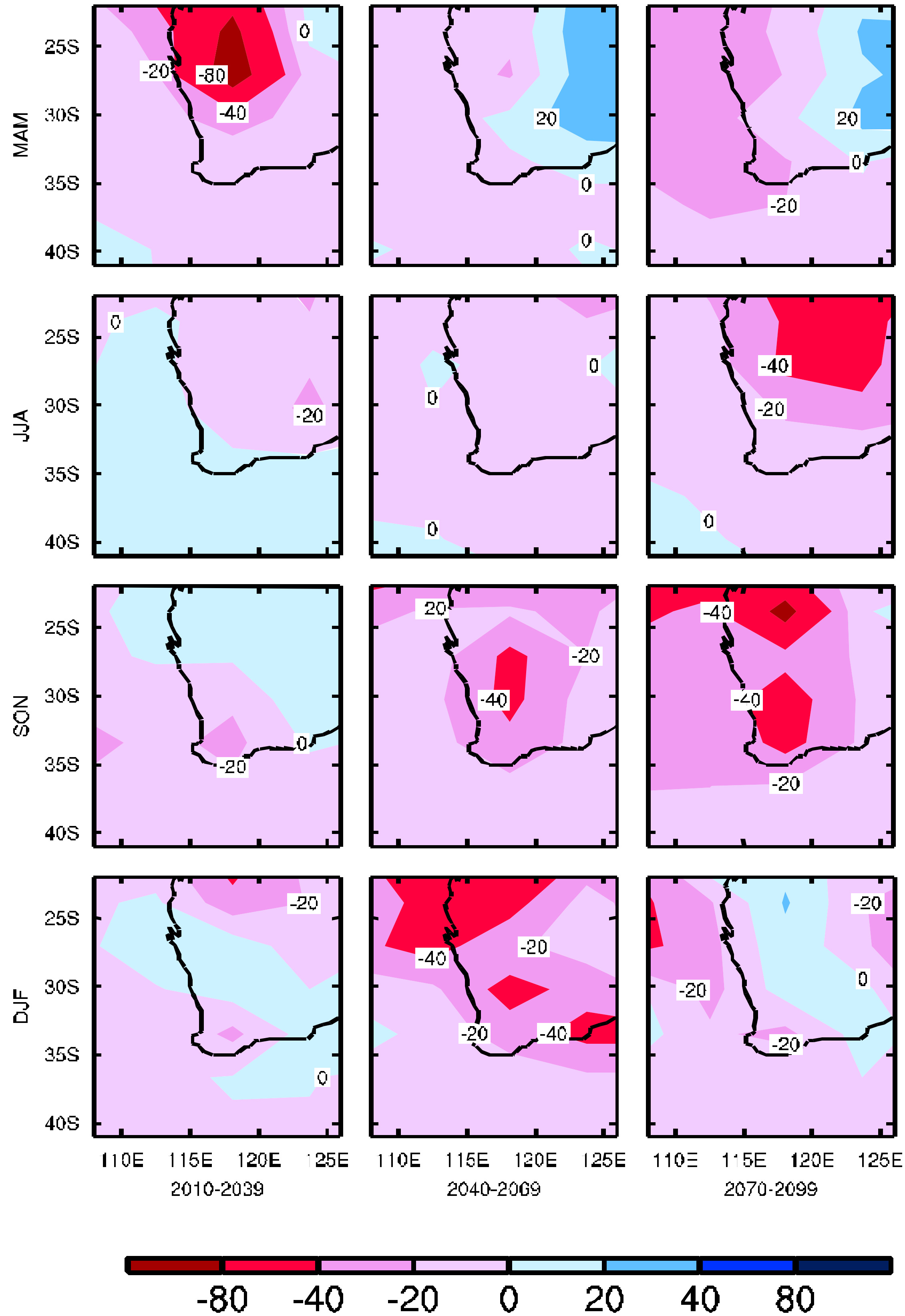

Figure 28: Aerosol CSIRO MARK 2 GCM BAU simulations of percentage changes in seasonal mean rainfall over SWA in the 2010-2039, 2040-2069 and 2070-2099 epochs. Seasons are autumn (MAM), winter (JJA), spring (SON) and summer (DJF). Rainfall is in % changes from the 1961-2000 climatology, with the colour bar on the figure showing the rainfall contour values.

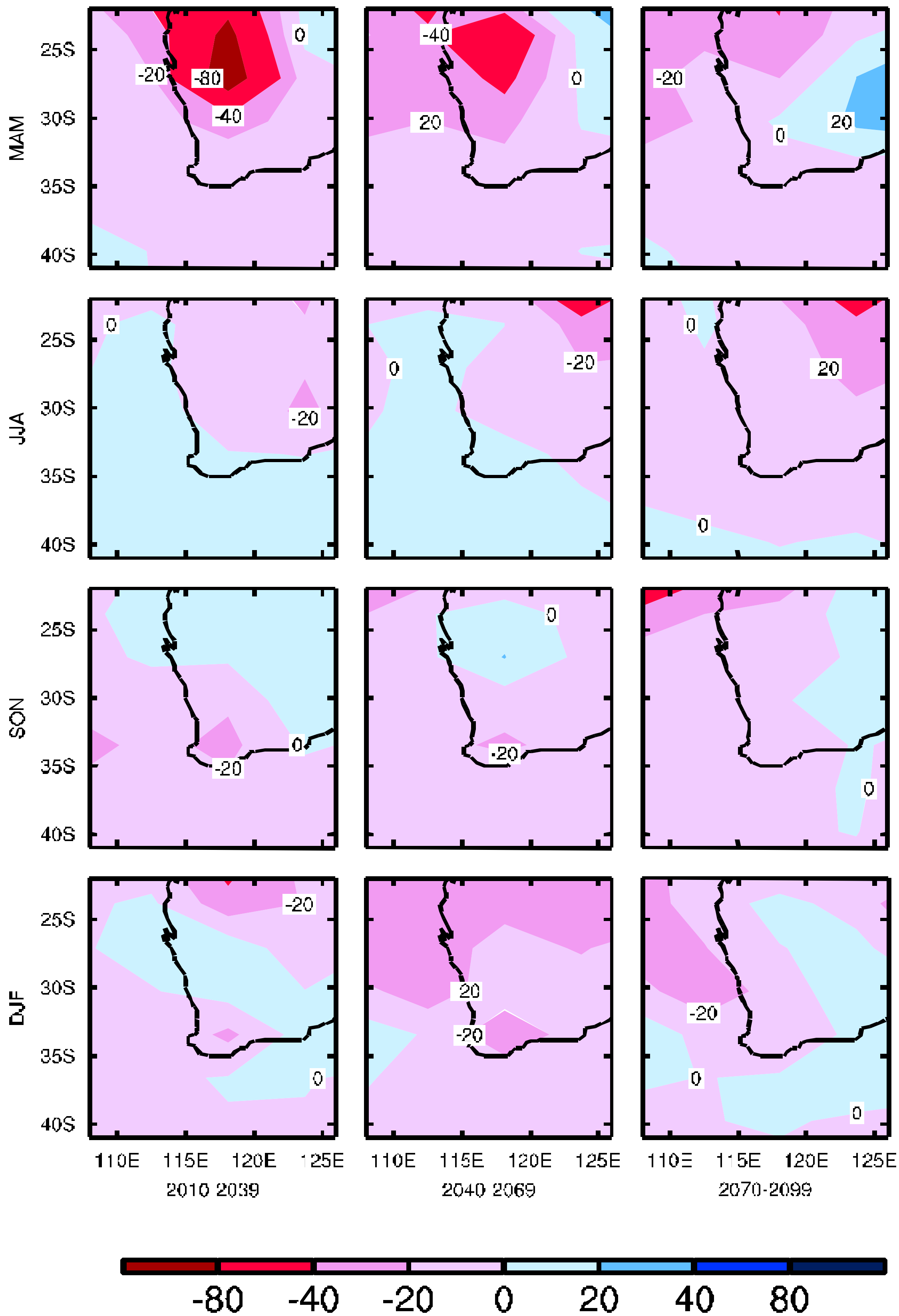

Figure 29: Aerosol CSIRO MARK 2 GCM PL simulations of percentage changes in seasonal mean rainfall over SWA in the 2010-2039, 2040-2069 and 2070-2099 epochs. Seasons are autumn (MAM), winter (JJA), spring (SON) and summer (DJF). Rainfall is in % changes from the 1961-2000 climatology, with the colour bar on the figure showing the rainfall contour values.

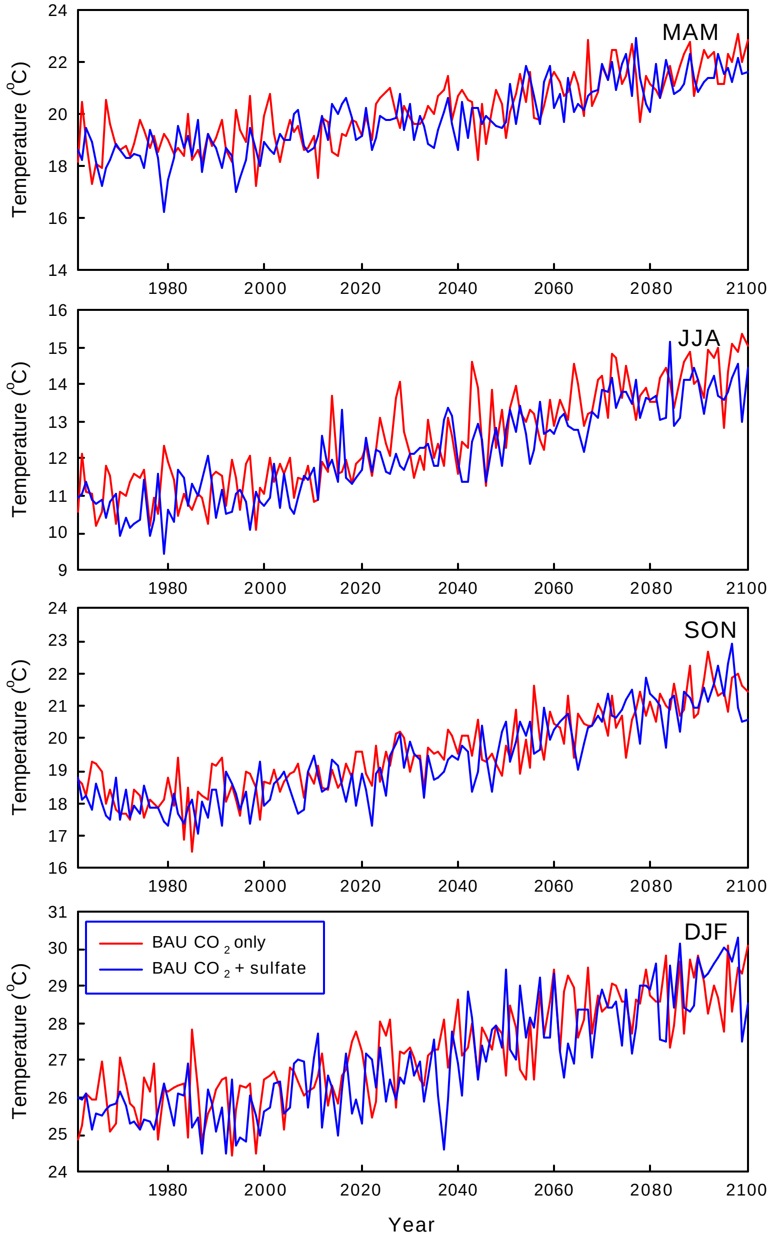

Figure 30: Wider SWA region time series of seasonal mean surface temperature for BAU CO_2 concentration scenarios from CSIRO Mark 2 GCM simulations run both with aerosols (sulphate) and without aerosols up to the year 2100. Surface temperature is in °C.

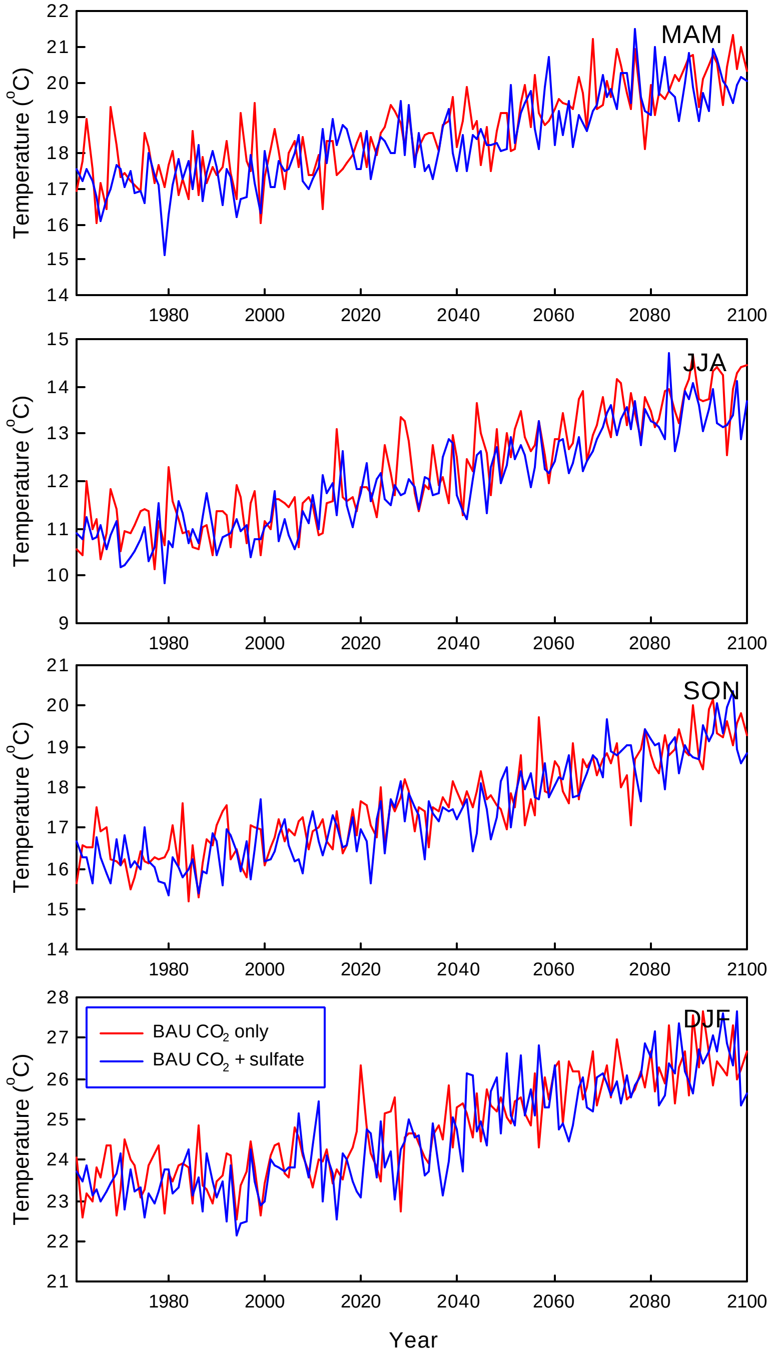

Figure 31: Land only SWA region time series of seasonal mean surface temperature for BAU CO_2 concentration scenarios from CSIRO Mark 2 GCM simulations run both with aerosols (sulphate) and without aerosols up to the year 2100. Surface temperature is in °C.

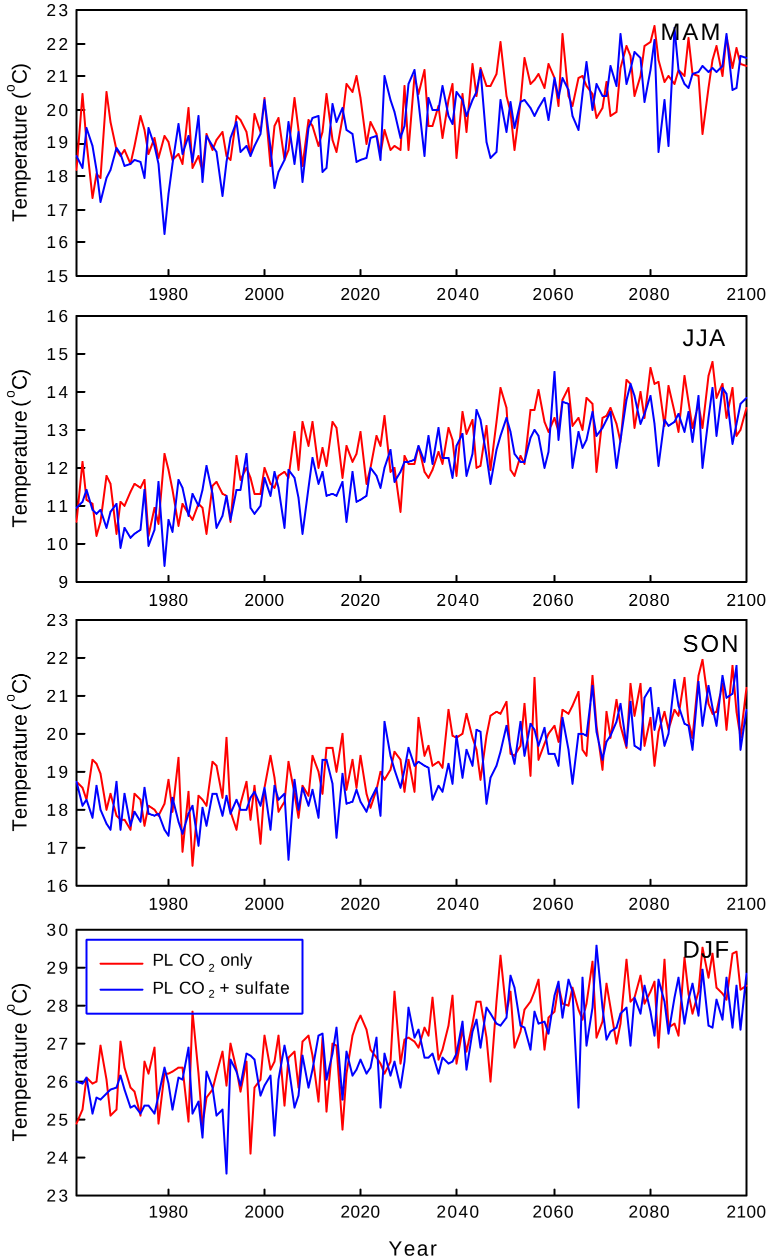

Figure 32: Wider SWA region time series of seasonal mean surface temperature for PL CO_2 concentration scenarios from CSIRO Mark 2 GCM simulations run both with aerosols (sulphate) and without aerosols up to the year 2100. Surface temperature is in °C.

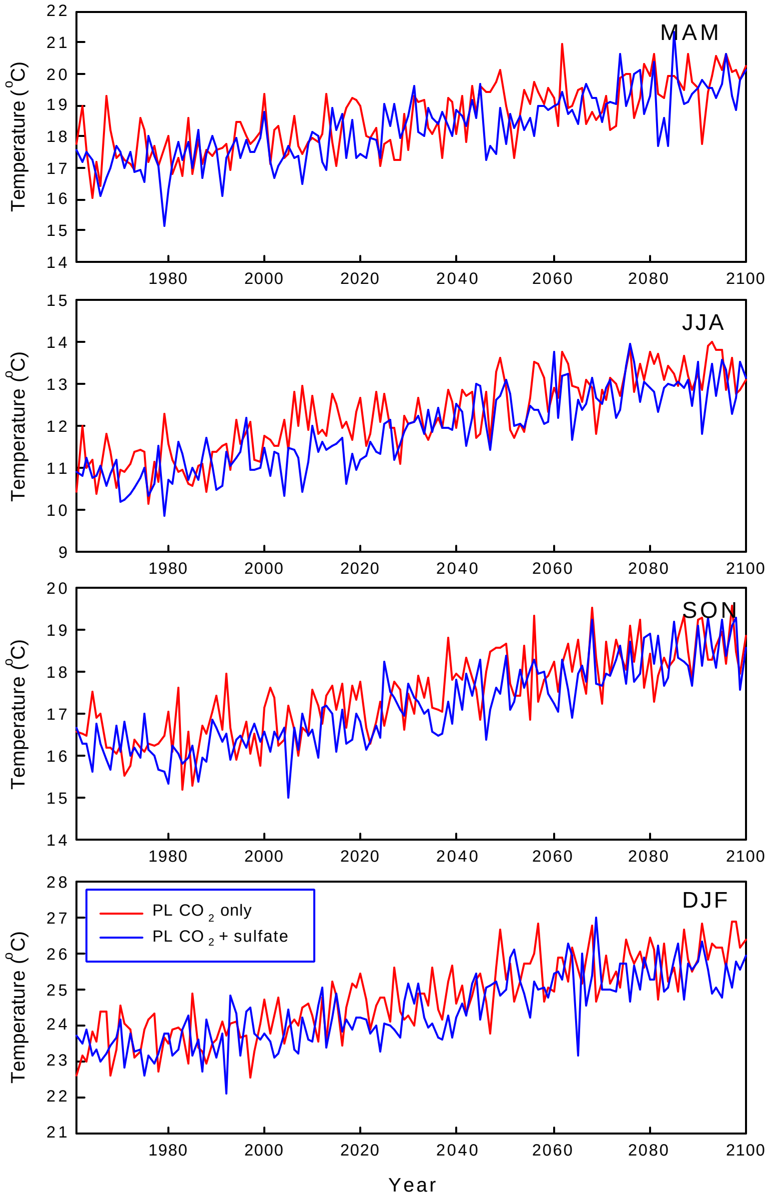

Figure 33: Land only SWA region time series of seasonal mean surface temperature for PL CO_2 concentration scenarios from CSIRO Mark 2 GCM simulations run both with aerosols (sulphate) and without aerosols up to the year 2100. Surface temperature is in °C.

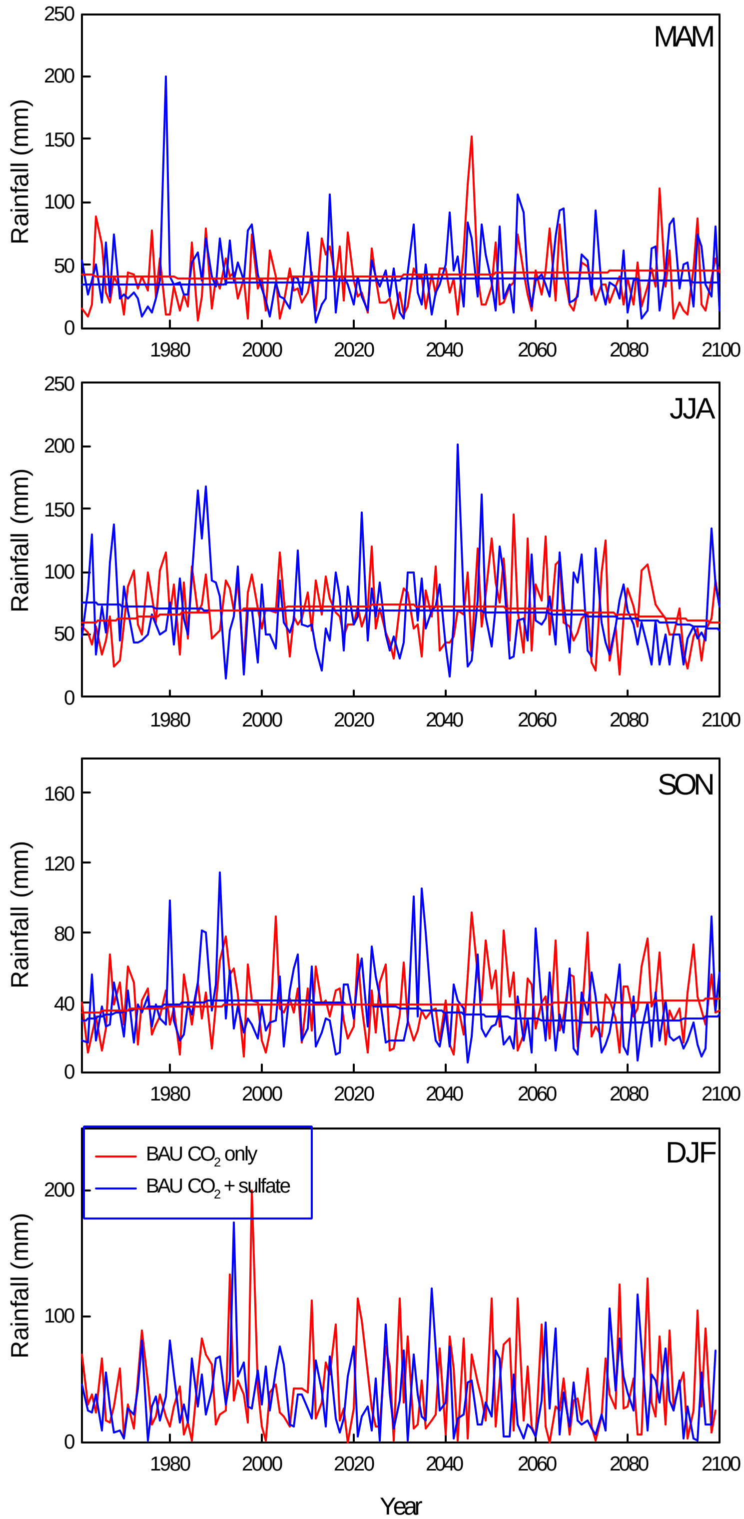

Figure 34: Wider SWA region time series of seasonal mean rainfall for BAU CO_2 concentration scenarios from CSIRO Mark 2 GCM simulations run both with aerosols (sulphate) and without aerosols up to the year 2100. The trend lines shown are 3rd order polynomial fits to the data where possible. Rainfall is in mm.

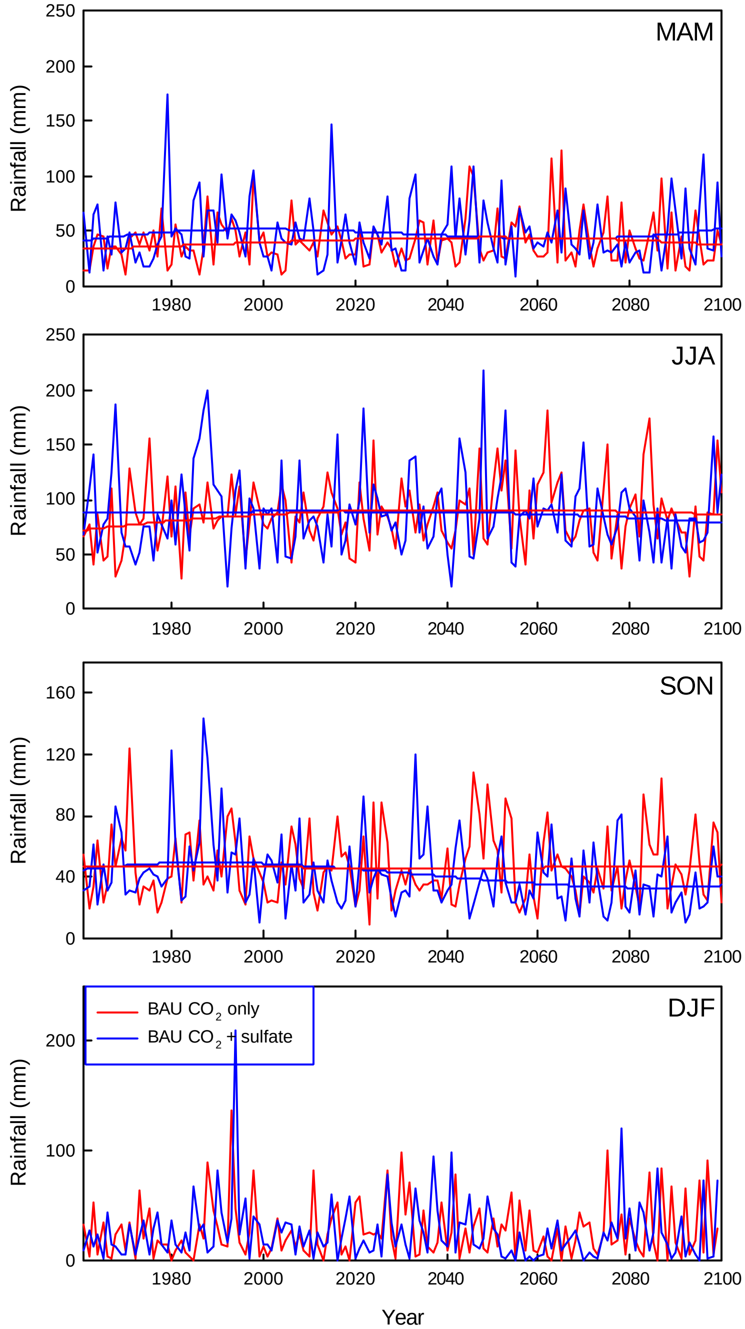

Figure 35: Land only SWA region time series of seasonal mean rainfall for BAU CO_2 concentration scenarios from CSIRO Mark 2 GCM simulations run both with aerosols (sulphate) and without aerosols up to the year 2100. The trend lines shown are 3rd order polynomial fits to the data where possible. Rainfall is in mm.

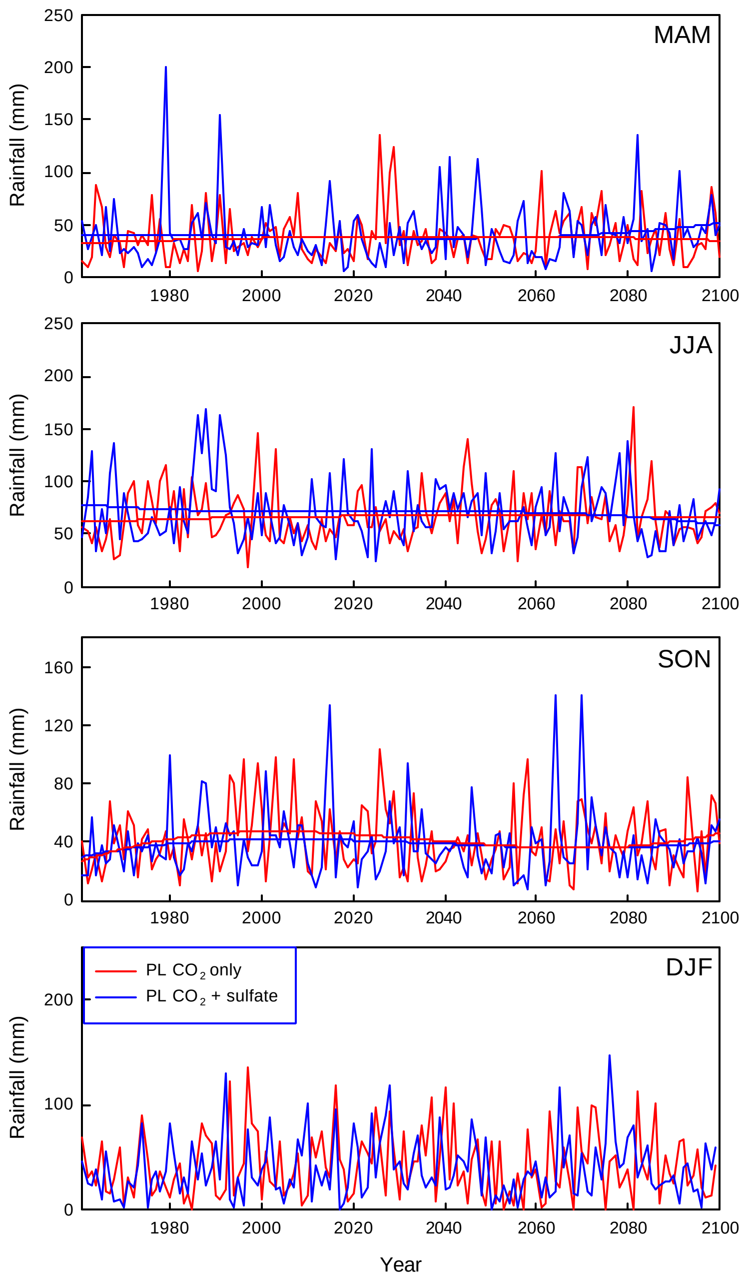

Figure 36: Wider SWA region time series of seasonal mean rainfall for PL CO_2 concentration scenarios from CSIRO Mark 2 GCM simulations run both with aerosols (sulphate) and without aerosols up to the year 2100. The trend lines shown are 3rd order polynomial fits to the data where possible. Rainfall is in mm.

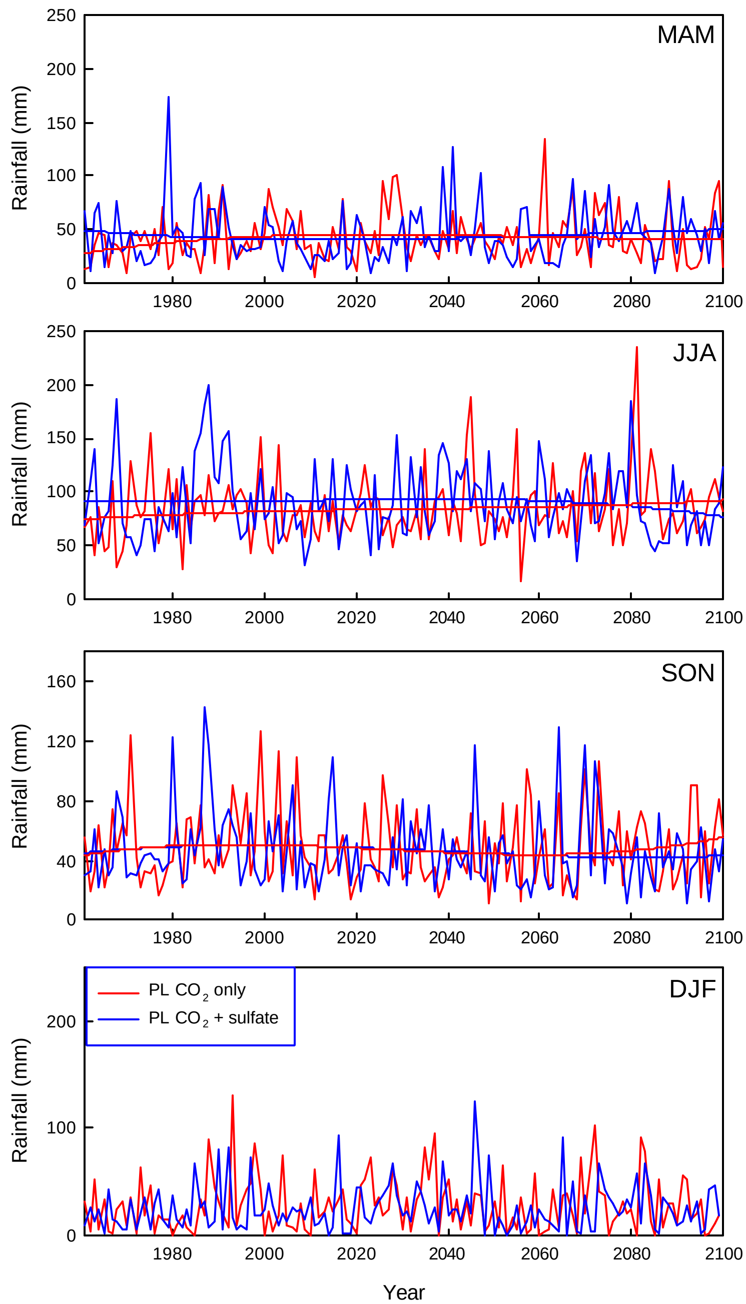

Figure 37: Land only SWA region time series of seasonal mean rainfall for PL CO_2 concentration scenarios from CSIRO Mark 2 GCM simulations run both with aerosols (sulphate) and without aerosols up to the year 2100. The trend lines shown are 3rd order polynomial fits to the data where possible. Rainfall is in mm.

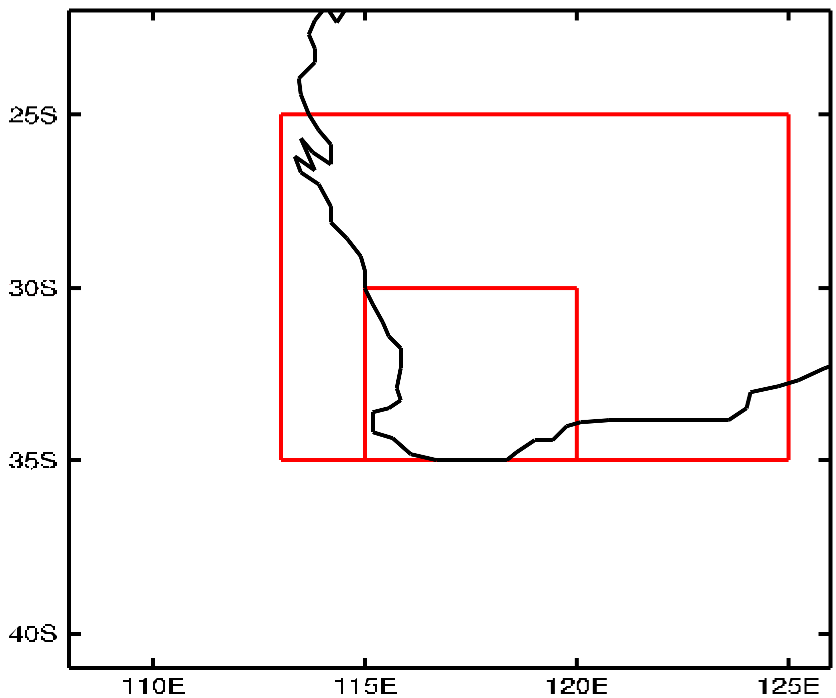

Figure 38: Wider and land-only regions of SWA examined in the DARLAM simulations

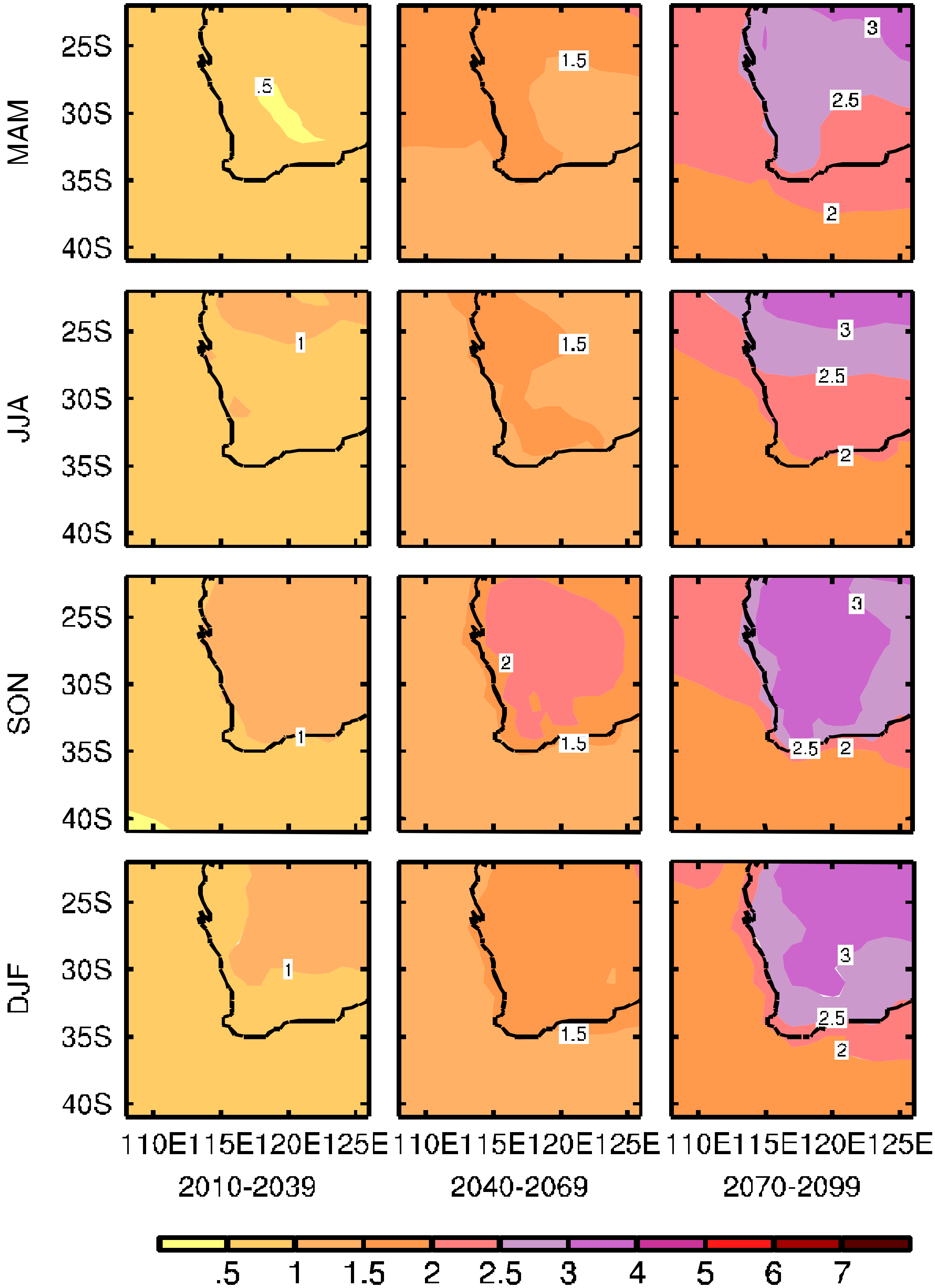

Figure 39: DARLAM simulations of annual mean surface temperature change over SWA in the 2010-2039, 2040-2069 and 2070-2099 epochs. Seasons are autumn (MAM), winter (JJA), spring (SON) and summer (DJF). Surface temperature is in °C from the 1961-2000 climatology, with the colour bar on the figure showing the rainfall contour values.

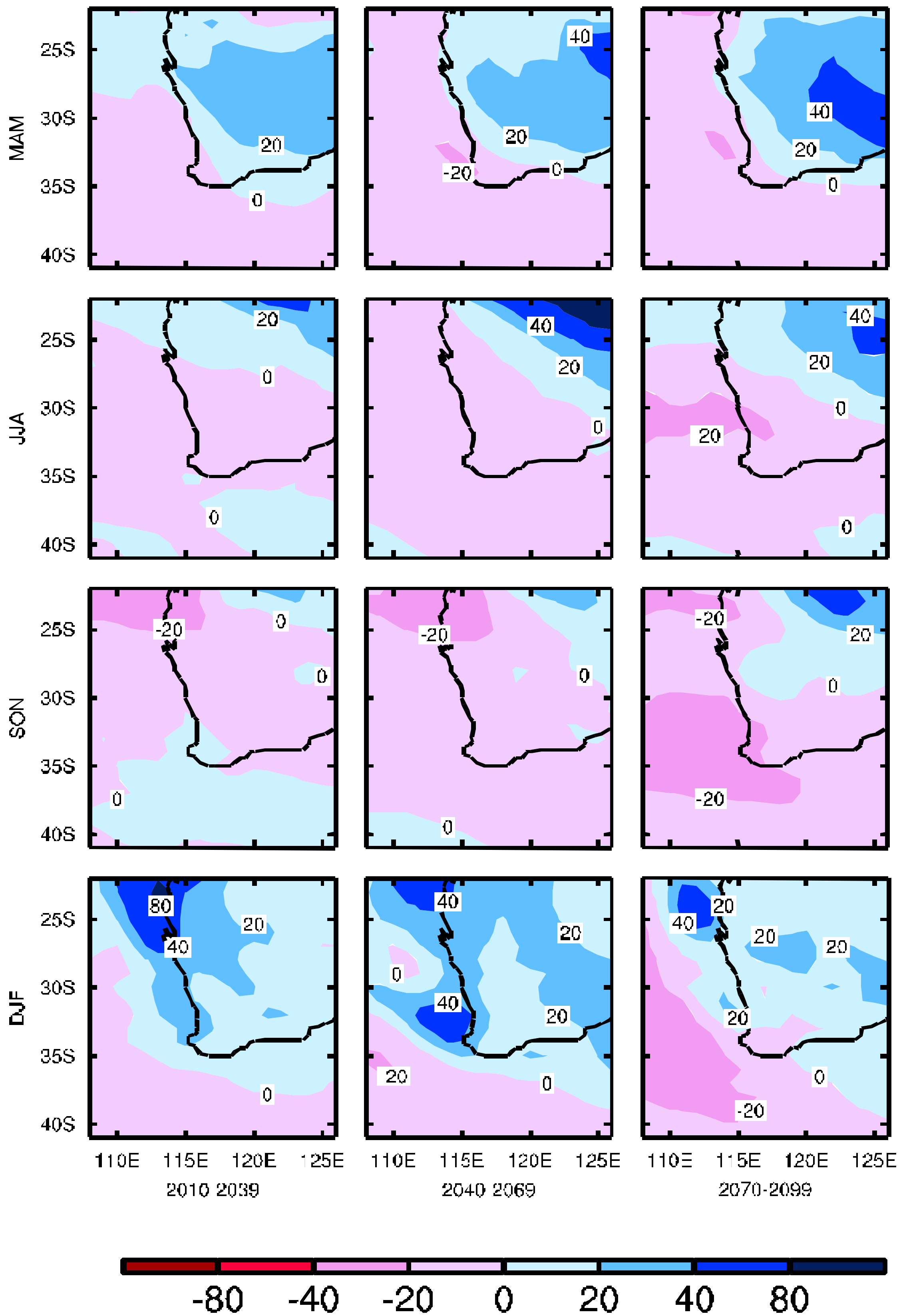

Figure 40: DARLAM simulations of percentage changes in seasonal mean rainfall over SWA in the 2010-2039, 2040-2069 and 2070-2099 epochs. Seasons are autumn (MAM), winter (JJA), spring (SON) and summer (DJF). Rainfall is in % changes from the 1961-2000 climatology, with the colour bar on the figure showing the rainfall contour values.

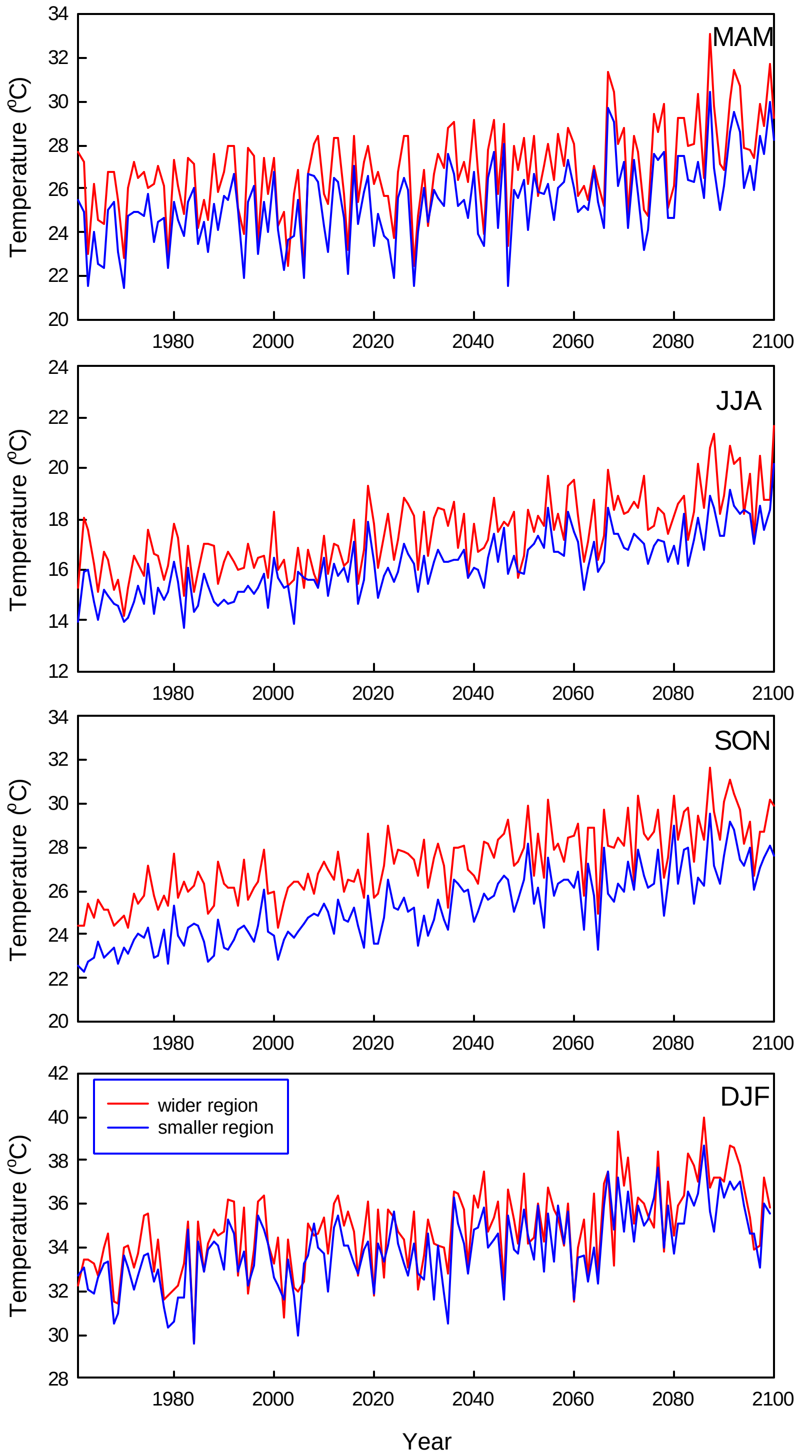

Figure 41: Time series of DARLAM simulations of seasonal mean maximum surface temperature over SWA up to the year 2100. Surface temperature is in °C, and is shown for the wider and smaller regions of SWA.

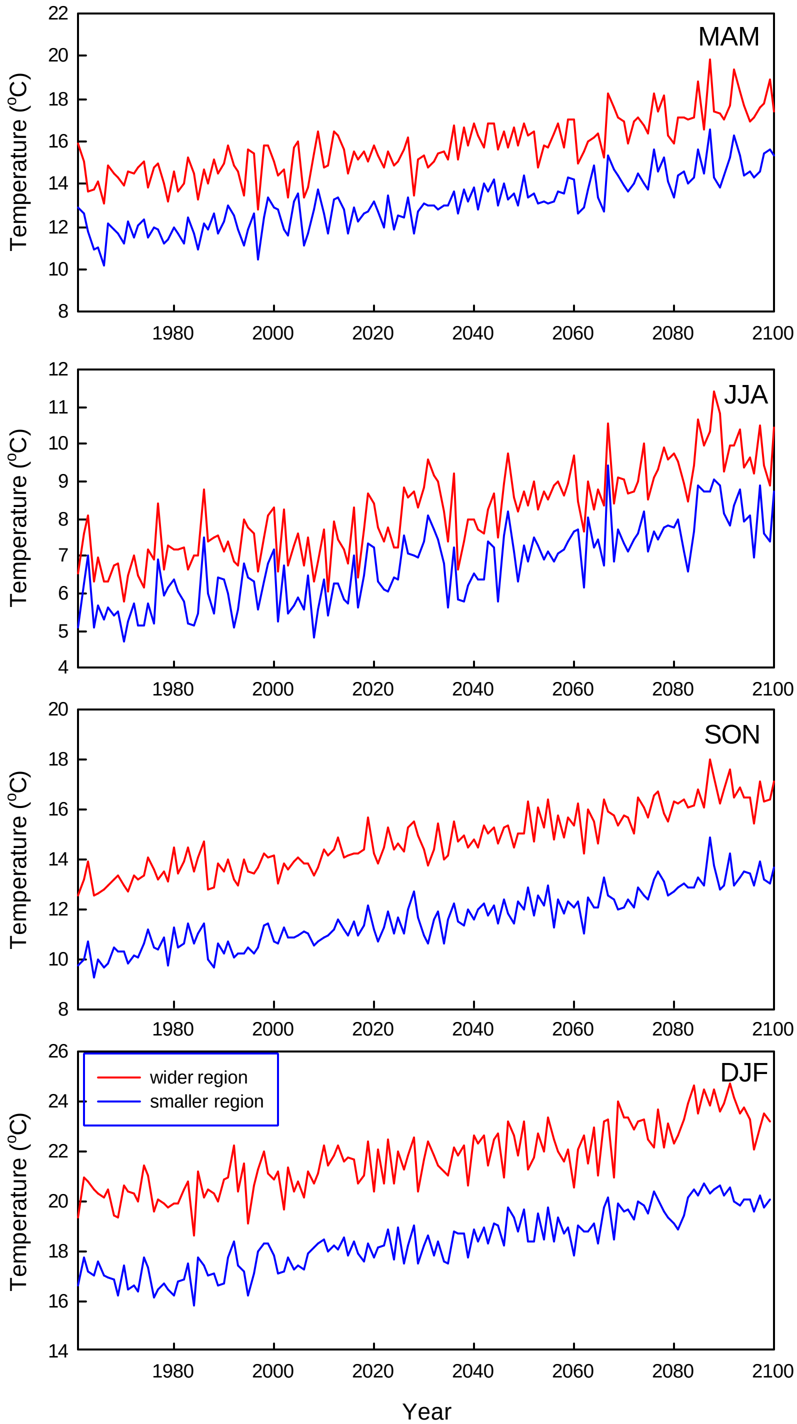

Figure 42: Time series of DARLAM simulations of seasonal mean minimum surface temperature over SWA up to the year 2100. Surface temperature is in °C, and is shown for the wider and smaller regions of SWA.

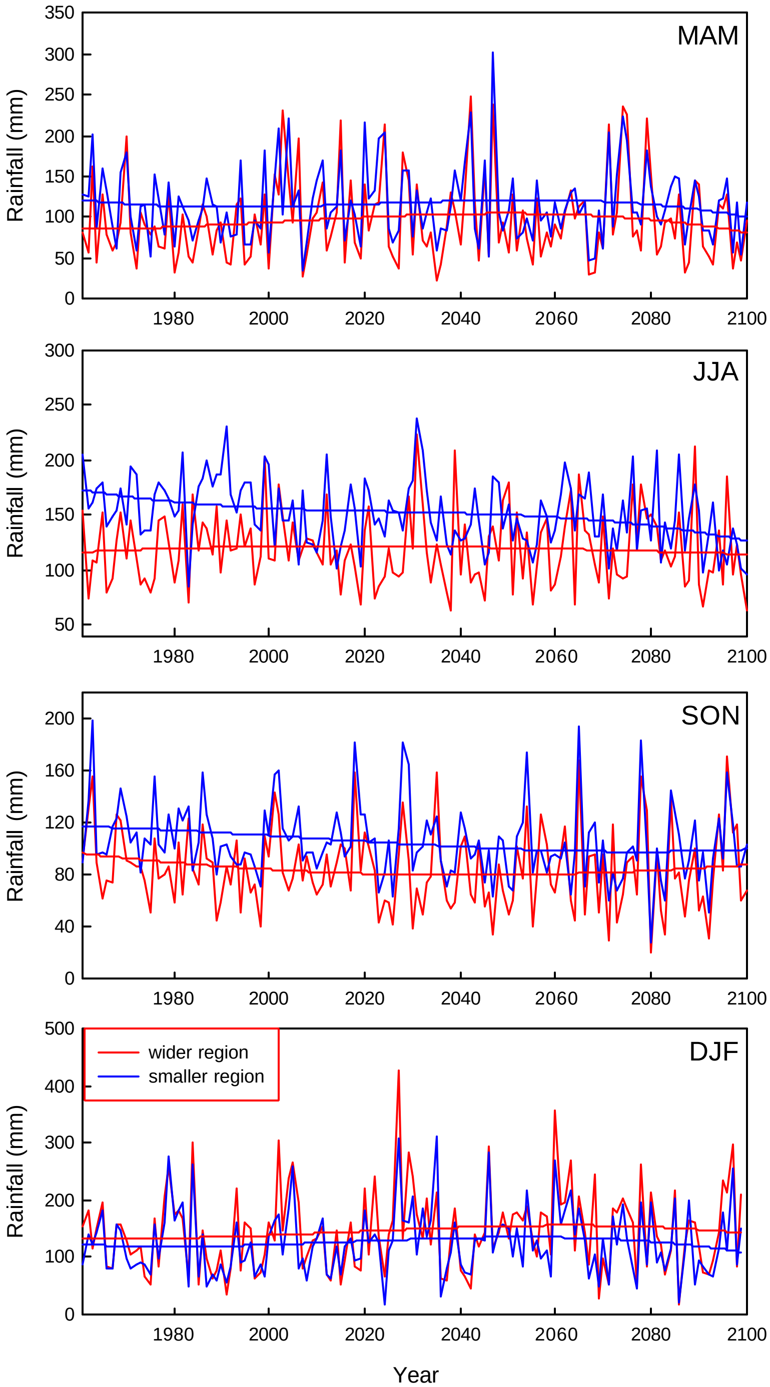

Figure 43: Time series of DARLAM simulations of seasonal mean rainfall over SWA up to the year 2100. The trend lines shown are 3rd order polynomial fits to the data. Rainfall is in mm, and is shown for the wider and smaller regions of SWA.